Universitat Autònoma de Barcelona

Institut Català de Nanociència i Nanotecnologia

BACHELOR'S DEGREE FINAL PROJECT

TOWARDS BIOFUNCTIONALIZED NANO-OPTO-ELASTIC SENSORS

PAU GÜELL GRAU
SCIENCE FACULTY
NANOSCIENCE AND NANOTECHNOLOGY DEGREE
JUNE 2014
DIRECTOR: BORJA SEPÚLVEDA (ICN2)

TABLE OF CONTENTS

1. INTRODUCTION 3

2. FABRICATION OF POLYMER NANOPILLAR ARRAYS 5

2.1. SILICON MASTER FABRICATION 6

2.1.1. NANOPILLAR DETAILS 7

2.2. PDMS FABRICATION (NEGATIVE MOULD) 8

2.3. NANOPILLAR FABRICATION 9

2.3.1. POLYMER DESCRIPTION 9

2.3.2. FABRICATION PROCEDURE 10

2.3.3. OPTIMIZED PROTOCOL 16

2.3.4. RESULTS 16

3. CHARACTERIZATION 23

3.1. ELASTIC CONSTANT 23

3.1.1. RESULTS AND DISCUSSION 23

3.2. CONTACT ANGLE 24

4. LSPR 25

4.1. EXPERIMENTAL SETUP 26

4.2. RESULTS AND DISCUSSION 27

5. MICROFLUIDICS 28

5.1. MICROFLUIDICS DESIGN 28

6. CONCLUSIONS 29

7. FUTURE PERSPECTIVES 29

8. ACKNOWLEDGEMENTS 30

9. REFERENCES 30

ANNEX 32

1. SILICON NANOPILLARS (SEM IMAGES): 32

2. POLYMER NANOPILLARS REPLICA (SEM IMAGES) 34

3. NANOPILLAR DIMENSION HISTOGRAMS 38

4. PEPTIDE DATA-SHEET 40

1. INTRODUCTION

MOTIVATIONS

Membrane receptors are essential for a huge range of functions of living cells[1]. They are the responsible to interact with the extracellular environment and with other cells. The interaction between membrane receptors and ligands is the starting point of molecular cascades which lead to different cellular responses. Membrane receptors have high importance in drug discovery due to its role as pharmacological targets[2]. Nonetheless, membrane receptors are very difficult to study: they are very difficult to isolate and purify out of the cellular membrane without altering their functions. Moreover, it is not possible to study the biochemical responses of an isolated membrane receptor outside the microenvironment of the cell membrane, so it would be very interesting to be able to study the interaction between membrane receptors and ligands in a living cell. Currently, detection methods of membrane receptor – ligand interactions are based on the introduction of fluorescence markers or genetic modifications, which may vary the membrane receptor functions[3,4].

On the other hand, the current drug screening assays does not take into account the physiological biomechanical environment, which is very different from current in-vitro assays. Increasing evidence shows that genetics and biochemistry alone cannot explain important biological phenomena. Moreover, the biomechanical environment surrounding the cells can be drastically altered in many diseases. For example, changes in the mechanical properties of the extracellular matrix and cells are strongly related in cancer development and metastasis[5-7]. Furthermore, the extracellular matrix may act as a mechanical ligand which can triggers different molecular cascades, even stem cell differentiation[8].

Therefore, a sensing platform which collects biochemical and biomechanical information on the interactions between membrane receptors and ligands in living cells in an adjustable biomimetic environment could revolutionize modern drug screening.

Here is presented a biomimetic sensing platform formed by polymer nanopillar arrays, where their mechanical properties can be modulated by their size and composition. Nanoplasmonic structures, consisting on gold nanodisks capping the nanopillars, are used for a label-free detection of the interactions between membrane receptors and ligands by refractometric Localized Surface Plasmon Resonance (LSPR). Then, they are functionalized with amino acid sequences of extracellular matrix proteins to attach the cells. Finally, all the system is integrated in a microfluidic system.

PREVIOUS KNOWLEDGE

Several studies has tried to mimic the biomechanical environment of the extracellular matrix using micropillars[9-12]. However, it is necessary to go down to the nanometre scale, since micropillars cannot mimic biological tissues, due to their large dimension and separation (allowing only low density of micropillars). For that reason, nanopillars with diameters between 150 and 200 nm and heights between 400 and 1500 nm are needed. Different tissues can be mimicked by only changing the aspect ratios of nanopillars and its composition, which will modify their elastic constant and their effective Young modulus[13] (equations 1 -2 , table 1).

Tissue	Effective Young Modulus
Brain	100 Pa
Liver	1 kPa
Muscle	10 kPa
Cartilage	100 kPa
Bone	1 MPa

TABLE 1. CORRELATION BETWEEN BIOLOGICAL TISSUES AND THEIR EFFECTIVE YOUNG MODULUS[13].

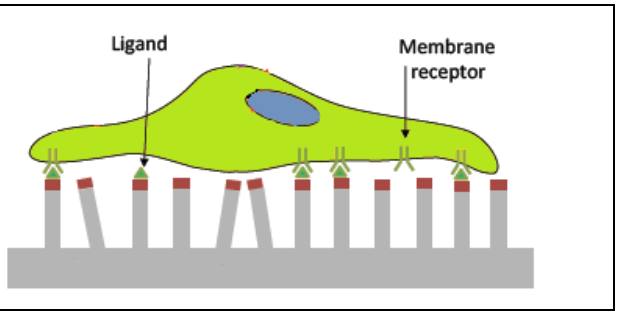

FIGURE 1. SCHEMATIC REPRESENTATION OF THE BIOMIMETIC ARRAY OF NANOPILLARS

$$K = \frac{3}{4}\pi E \frac{r^4}{L^3}$$

EQUATION 1. ELASTIC CONSTANT EQUATION[13]

$$E_{eff} = \frac{9k}{4\pi r}$$

EQUATION 2. EFFECTIVE YOUNG MODULUS EQUATION[13]

A wide range of label-free detection methods are used nowadays, from mechanical (Quartz Crystal Microbalance[15], microcantilevers[16]…) to optical sensors (SPR[17], Mach-Zehnder[18]…). However, a transduction method which allow a real-time, label-free, non-invasive detection with sub-micrometer spatial resolution it is necessary for this application. For that reason, nanoplasmonics, and specifically refractometric (LSPR) will be used in this work due to its unique sub-micrometer spatial resolution, the improvement in sensibility and its multiplexing capabilities, comparing to conventional optic sensors[19]. When LSPR is excited, the absorption and scattering of photons are strongly enhanced, and very intense electromagnetic fields are confined around the nanoparticles. The resonance wavelength highly depends on the refractive index of the external medium and the penetration of the electromagnetic field is 20 to 40 nm, making these sensors especially suitable for detection in living cells.

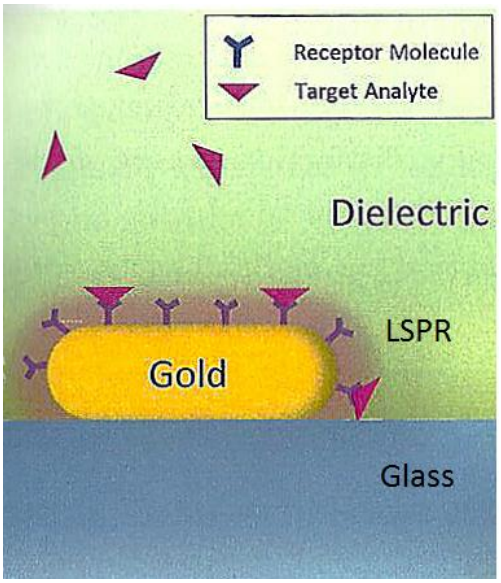

FIGURE 2. SCHEMATICS REPRESENTING THE SENSING PRINCIPLE OF REFRACTOMETRIC LSPR SENSING USING A SUB-WAVELENGTH METALLIC NANOPARTICLE[14]

In order to perform an effective attachment between the nanopillars and the cells, nanopillars should be functionalized with recognition sequences of extracellular matrix proteins. Since the nanopillars are capped with a gold nanodisk, they can be functionalized by taking advantage of the reaction between gold and a thiol group, which is well-known and widely-used for biofunctionalization[20,21].

Furthermore, due to the nanofabrication techniques, this is also a low-cost sensor and it would be easy to produce in large scale.

Therefore, the proposed innovative nano-opto-elastic platform of a polymeric nanopillar array with LSPR detection is a low-cost and easy to produce in large scale biomimetic sensor, which will provide biochemical and biomechanical information of membrane receptor–ligand interactions in living cells, using a label-free, real-time, non-invasive optical transduction technique with sub-micrometer resolution and multiplexing capabilities. This platform will open the path for the development of the novel label-free opto-mechanical biosensing scheme, based on the simultaneous local refractive index sensing and opto-mechanical actuation of the elastic nanopillars[22,23].

OBJECTIVES

In this work are presented the first steps of the design of the presented nano-opto-elastic sensor. Specifically, the aims of this work are i) the optimization of the polymeric nanopillar array fabrication, using soft-lithography techniques to replicate a silicon master of nanopillars; ii) the characterization of the replicated nanopillars by SEM and contact angle measurements; iii) initial studies by LSPR about biofunctionalization; iv) the first design of the microfluidic system which will embed the sensing platform.

2. FABRICATION OF POLYMER NANOPILLAR ARRAYS

The fabrication of polymer nanopillar arrays is based on a soft-lithography replica-moulding process, which uses arrays of silicon nanopillars as masters and elastomer silicone moulds to make the replicas.

The fabrication process is divided in the following steps (see Figure 2):

1. Fabrication of the silicon masters by metal-assisted wet chemical etching
2. Fabrication of the elastomer polydimethylsiloxane (PDMS) moulds
3. Replication of the polymer nanopillars using photo-curable epoxies
4. High directional metal evaporation to form the nanoplasmonics caps

This is a low-cost, straight-forward and large scale fabrication method obtain large areas of arrays of polymer nanopillars.

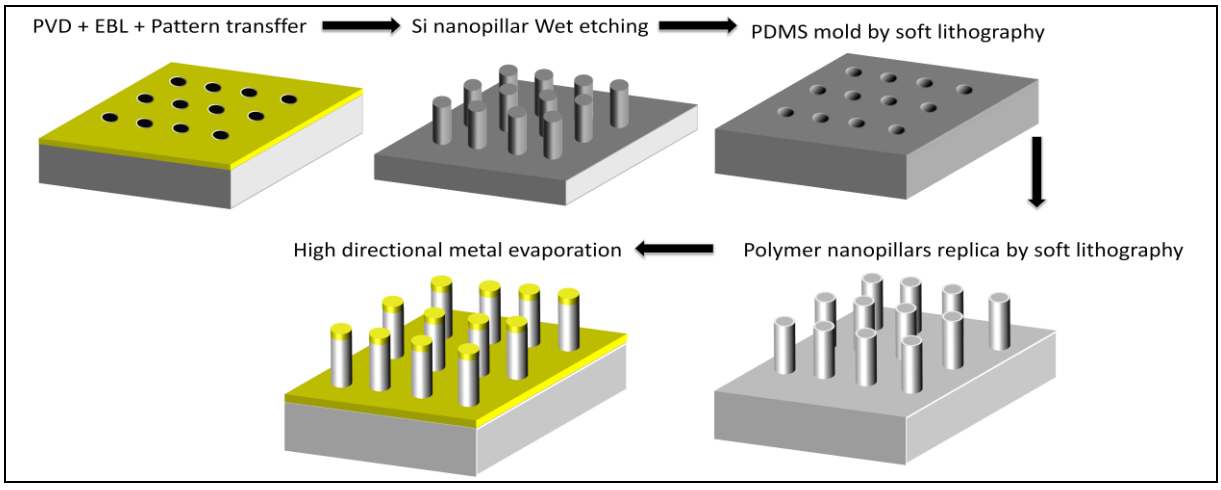

FIGURE 3. SCHEMATIC REPRESENTATION OF THE POLYMERIC NANOPILLAR FABRICATION

Currently, the fabrication protocol of the silicon master and the PDMS mould are optimized. Therefore, this section is focused on the optimization of the fabrication of polymeric nanopillar replica.

2.1. SILICON MASTER FABRICATION

The master that will be used to replicate in different polymers are silicon nanopillar arrays. To fabricate nanopillars on silicon wafers a metal assisted wet chemical etching method is used. Since this is an electrochemical reaction catalyzed by gold, a gold film with nanoholes must be patterned on the silicon wafer. In this etching process, the silicon etching rate is fast below the metal and very slow in the absence of gold. Therefore, this process leads to the formation of columnar silicon nanostructures.

To achieve the initial gold layer with nanoholes, shadow nanosphere lithography and electron-beam evaporation are used, which allows the control of the diameter and the separation between nanopillars (see Figure 4).

It is crucial to fabricate accurately this silicon mould because all the errors in the silicon master will be replicated. The fabrication protocol of the silicon master is the following:

SHADOW NANOSPHERE LITHOGRAPHY

Polystyrene (PS) nanospheres of 300 nm or 400 nm of diameter have been used. Their diameter provides the separation distance between the nanopillars. The nanospheres are spread at the interface between water and air in a Petri dish (approximately covering 70% of the surface), where nanospheres adopt a self-organized hexagonal close-packed arrangement.

Then, a silicon wafer is put below the nanospheres and the liquid is extracted. When all the liquid is extracted, PS nanospheres are deposited on the surface of the silicon wafer.

RIE

To precisely control the diameter of the nanopillars, Oxygen Reactive Ion Etching (RIE) is used. Oxygen RIE isotropically etches the PS nanospheres on the silicon surface, reducing their diameter. The final diameter of the nanospheres determines the diameter of the nanopillars.

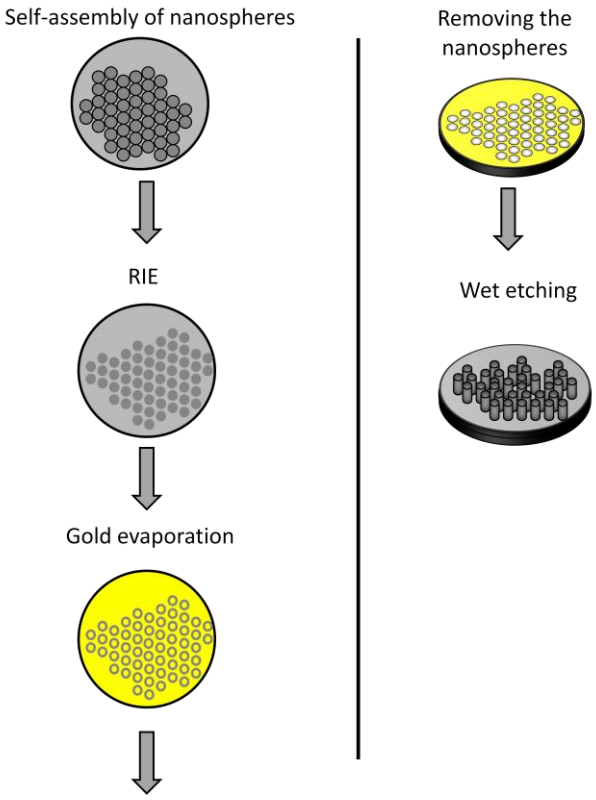

FIGURE 4. SCHEMATIC REPRESENTATION OF THE SILICON MASTER FABRICATION PROCESS

E-BEAM EVAPORATION

Gold is necessary in this protocol because it is the catalyst of the wet etching reactions. Electron-beam evaporation is used for evaporating gold and titanium on the surface. Firstly, titanium was evaporated making a layer of 0,5 nm. This layer is used to stick the gold layer to silicon. After that, 19 nm thick gold layer was evaporated.

WET ETCHING

Wet etching is used to fabricate nanopillars on a silicon wafer with high control of their height.

Firstly, PS nanospheres are removed using adhesive tape. Then, wet etching is done using fluorhydric acid, hydrogen peroxide and deionised water. Silicon is oxidized by the hydrogen peroxide and is dissolved by the fluorhydric acid. These reactions are catalyzed by the gold surface. The areas where the nanospheres were previously situated do not have gold nor titanium, so this reaction does not happened and the silicon is not attacked, forming the nanopillars, organized in a hexagonal close-packed distribution. The height of the nanopillars can be controlled by the time of reaction.

Once the silicon master mould is fabricated, it can be used several times (between 10 and 15) for doing the replications.

2.1.1. NANOPILLAR DETAILS

In this work, three different sets of samples were used. The dimensions of nanopillars were different in each sample for obtaining different elastic constants and for demonstrating the limit of dimensions that nanopillars can be replicated successfully. Details of each sample are detailed in tables 2, 3, 4:

Sample	Diameter (nm)	Height (nm)	Separation between nanopillars (nm)	SEM
#1.1	179 ± 11	755 ± 87	300	Annex Image 1
#1.2	163 ± 13	496 ± 54	400	Annex Image 2
#1.3	151 ± 14	928 ± 56	400	Annex Image 3

TABLE 2. DETAILS OF THE SILICON NANOPILLARS. SAMPLES #1

Sample	Diameter (nm)	Height (nm)	Separation between nanopillars (nm)	SEM
#2.1	197 ± 15	592 ± 67	400	Annex Image 4
#2.2	194 ± 12	803 ± 50	400	Annex Image 5
#2.3	208 ± 6	1375 ± 322	400	Annex Image 6
#2.4	145 ± 13	1071 ± 104	400	Annex Image 7

TABLE 3. DETAILS OF THE SILICON NANOPILLARS. SAMPLES #2

Sample	Diameter (nm)	Height (nm)	Separation between nanopillars (nm)	SEM
#3.1	138 ± 8	489 ± 24	400	Annex Image 8
#3.2	133 ± 13	976 ± 50	400	Annex Image 9
#3.3	133 ± 14	1415 ± 116	300	Annex Image 10

TABLE 4. DETAILS OF THE SILICON NANOPILLARS. SAMPLES #3

2.2. PDMS FABRICATION (NEGATIVE MOULD)

The silicon master can be used several times to do a negative mould of PDMS for the replication of the silicon nanopillars with different polymers. PDMS is commonly used as a mould due to its high elasticity, low cost and its ease of use.

The fabrication of the PDMS mould is composed by the following steps: silanization of nanopillars to produce an anti-adherent surface, mix between PDMS and the cross-linker, deposition of the mixture on the silicon nanopillars, removing of air bubbles by vacuum and thermal curing.

SILANIZATION

Silicon master samples are put in a Petri dish. Nanopillars must be oxidized to produce chemical changes on the silicon surface, creating hydroxyl terminations, which will react with the silane, making the anti-adhesive monolayer. This non-sticking property is necessary to easily remove the PDMS from the silicon master.

The silicon nanopillar surface is oxidized by an oxygen plasma with the following conditions:

Power	75W
Gas flow	15%
Time	2 minutes

TABLE 5. OXYGEN PLASMA CONDITIONS FOR THE SILANIZATION PROCESS

Then, the silane layer is created by vapour phase silanization: the samples are put in a vacuum chamber with an opened Eppendorf tube containing 50 µL of (tridecafluoro-1,1,2,2-tetrahydrooctyl)trichlorosilane and vacuum is made during 30 minutes. After that, the vacuum pump is stopped and the vacuum chamber is closed during 1 hour and 30 minutes. During this time, the silane, which has been evaporated, starts to fall on the nanopillar surface, producing the desired monolayer, which will have the non-sticking property because of the fluoride terminations.

PDMS MIX

Separately, the mixture between PDMS and the cross-linker is made. The optimum ratio (by weight) between both components for our interests is 10:1. This ratio will modify the Young modulus of the resultant PDMS. It is important to mix vigorously to assure that the curative agent is well distributed. This mixture is put into a vacuum chamber and vacuum is made during approximately 20 minutes, which is the time needed for eliminating all the bubbles created during mixing.

DEPOSITING PDMS ON THE SAMPLES

Once the silanization is done, the PDMS is mixed and the bubbles are eliminated, the PDMS is deposited on the Petri dish with the samples. The liquid PDMS must cover all the Petri dish, making a layer of 2 mm thick. It is important that the PDMS must not fall directly on the samples, because it can damage the samples, making the nanopillars fall. It is useful to use carefully a nitrogen gun for spreading all the PDMS uniformly through the Petri dish.

Then, the Petri dish is put in the vacuum chamber and the vacuum is made during 1 hour. This is another crucial step, which will help to eliminate the rests of air which remain within the PDMS, helping the PDMS to fill all the structure of the sample for a proper replication.

CURING

After eliminating the bubbles for 1 hour, the PDMS has to be cured, by putting the Petri dish on the Hot Plate for 1 hour at 100ºC. After that, the Petri dish is removed from the Hot Plate.

Once the Petri dish is cooled, the PDMS can be removed from the samples. Firstly, a general cut is made for separating the different samples which are stuck on the Petri dish. Then, the PDMS has to be removed carefully, holding it from one side and removing it to the other (see image 1). It is important to remove the PDMS very slowly and do not return the PDMS in its previous position. Otherwise, the nanopillars of the silicon masters can be damaged.

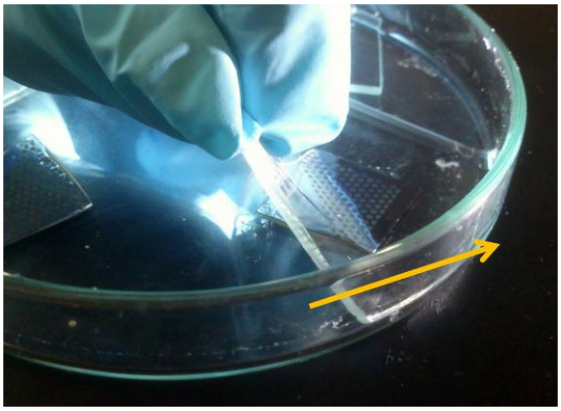

IMAGE 1. REMOVING THE PDMS. THE ARROW SHOWS THE DIRECTION OF DEMOLDING.

PDMS CHECK

A useful way to check if the PDMS mould has been fabricated correctly is to illuminate it. The regular matrix of nanoholes in the PDMS diffracts visible light and a different range of colours can be seen depending on the angle of incidence of light (Images 2 and 3).

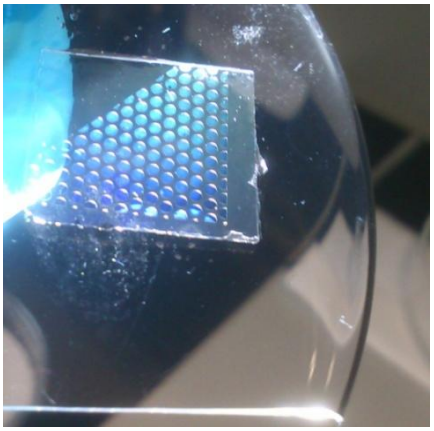

IMAGE 2. DIFFRACTION OF LIGHT DUE TO NANOHOLES. SAMPLE OF NANOPILLARS WITH 400 NM OF SEPARATION

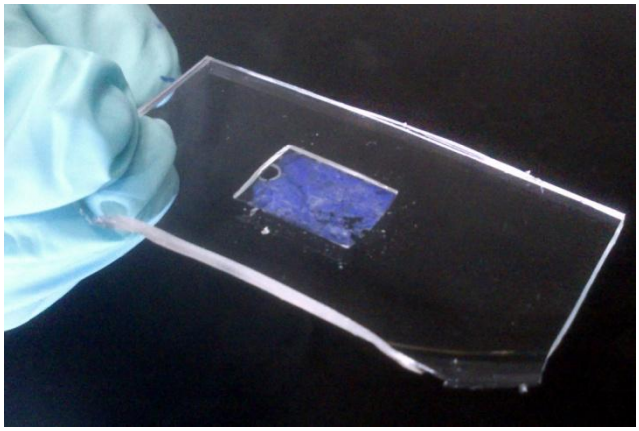

IMAGE 3. DIFFRACTION OF LIGHT DUE TO NANOHOLES. SAMPLE OF NANOPILLARS WITH 300 NM OF SEPARATION

2.3. NANOPILLAR FABRICATION

The next step is making the nanopillar replica using photocurable polymers. In this work two different photopolymer have been used: EPO-TEK® OG142-87 and EPO-TEK® OG603.

2.3.1. POLYMER DESCRIPTION

EPO-TEK® OG142-87 is a single component, low viscosity, UV curable epoxy. The main information which can be extracted from the data sheet is the following:

Recommended Cure	100mW/cm @ 240-365 nm for >2 minutes Or 100mW/cm @ 300-500 nm for >2 minutes + 150ºC for 1 hour
Young Modulus	3590 GPa
Refractive index (cured)	1,5058 @ 589 nm

TABLE 6. EPO-TEK® OG142-87 DATA SHEET

EPO-TEK® OG603 is also a single component, low viscosity, UV curable epoxy. It is an all-purpose, general adhesive for optical applications. It meets the requirements of USP Class VI biocompatibility standards for medical implants. The main information which can be extracted from the data sheet is the following:

Recommended Cure	100mW/cm @ 240-365 nm for > 5 seconds
Young Modulus	1729 GPa
Refractive index (cured)	1,5037 @ 589 nm

TABLE 7. EPO-TEK® OG142-87 DATA SHEET

The recommended cure will be our reference when we start to work with this polymer. It is also important to know the Young modulus and the refractive index because we will need those values for the mechanical and optical characterization of the nanopillar structure.

2.3.2. FABRICATION PROCEDURE

The fabrication protocol has been optimized for replicating the silicon nanopillar arrays which have been described at tables 2, 3 and 4. It has to be taken into account that this procedure must be done under working conditions of absence of UV light.

Since both polymers are quite similar, both protocols have been optimized in parallel, so some steps in the protocol of one polymer has been corrected using information from the other polymer.

The fabrication protocol of nanopillars will consist on i) centrifugation of the polymer to eliminate bubbles, ii) weighting the correct amount of polymer for a proper replica, iii) applying vacuum to eliminate air remaining within the polymer and to help the polymer to penetrate into the PDMS nanoholes, iv) putting and pressuring the glass which will be the substrate of the nanopillars, v) curing with UV light and iv) thermal post-curing (figure 5). Below we explain the details and the optimizations that we have carried out in each step.

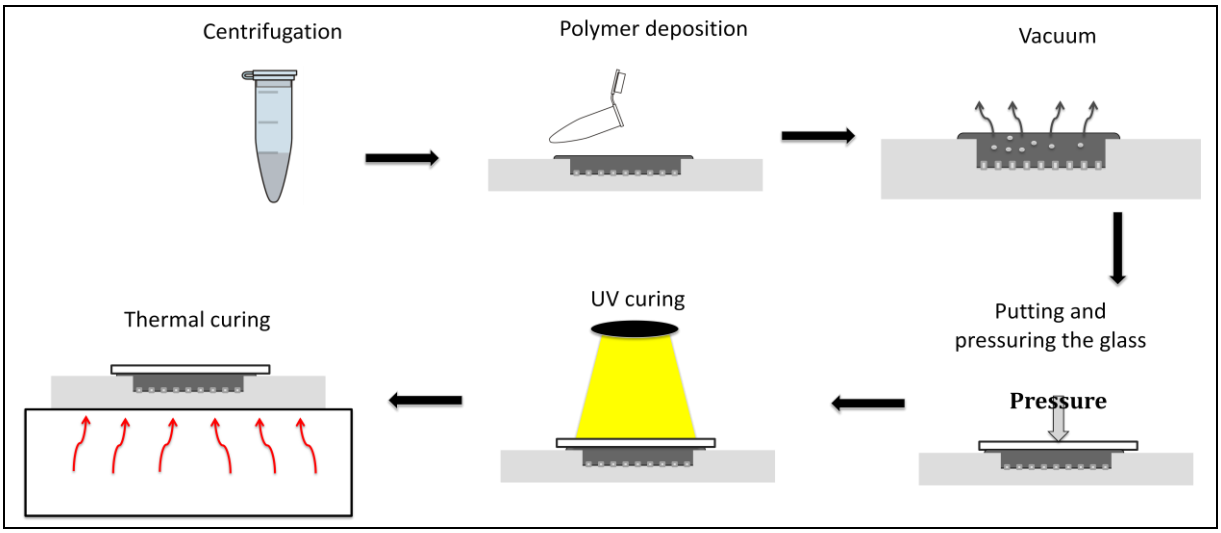

FIGURE 5. SCHEMATIC REPRESENTATION OF THE NANOPILLAR REPLICATION PROCESS

CENTRIFUGATION

A small quantity (approximately 1 mL) of polymer is put into an Eppendorf tube and is centrifuged for 5 minutes at 3000 rpm. The centrifugation helps to eliminate microbubbles which are within the liquid.

WEIGHTING THE POLYMER

The PDMS negative mould is put on a glass surface (for example, a Petri dish). It is possible (and useful) to put some moulds on the same Petri dish to replicate several samples in parallel.

The amount of polymer needed to cover all the sample depends on how large the sample is. There is not a formula to determine the amount of polymer needed, but the general rule is to fill the shape of the sample of the PDMS and not to put an excess of polymer. Otherwise, some problems appear: if there is not enough amount of polymer to fill the sample, the next step (vacuum) will not be useful. If happens the contrary and there is an excess of polymer, this excess will dirty the replication and can cause some problem while the nanopillars are removed from its mould.

VACUUM

Once the polymer have been poured out on the PDMS mould, it is necessary to assure that the polymer penetrates inside the nanoholes of the PDMS completely. This is one of the most important steps in this work, because is not evident that the polymer fills the holes. There are some rests of air within the polymer and inside the nanoholes, which has to be eliminated. For that reason, the PDMS mould with the polymer is put into the vacuum chamber and vacuum is done.

The time needed for a proper penetration of the polymer into the holes is dependent on the size of the holes: the smaller the holes are, the higher the time will be needed to completely fill them.

The time of vacuum in the first attempts was 30 seconds (trying to replicate the silicon samples #1). After carrying out the first experiments, two important events could be observed: on the one hand, both polymers were not stable to a continued vacuum (due to the low vapour pressure it starts to boil, creating new bubbles into the polymer), so we found out that it is more appropriate to do the vacuum with pulses of 5 or 10 seconds. Moreover, doing the vacuum in short pulses helps to move the polymer inside the nanoholes because in every pulse the pump applies a force due to the extraction of gas molecules inside the chamber. Nevertheless, the first SEM images (Image 5) showed that the polymer could not penetrate inside the nanoholes completely, implying that more time of vacuum was needed for both polymers.

IMAGE 4. DURING THE VACUUM, AIR IS ELIMINATED FROM INSIDE THE POLYMER, HELPING TO A BETTER REPLICATION

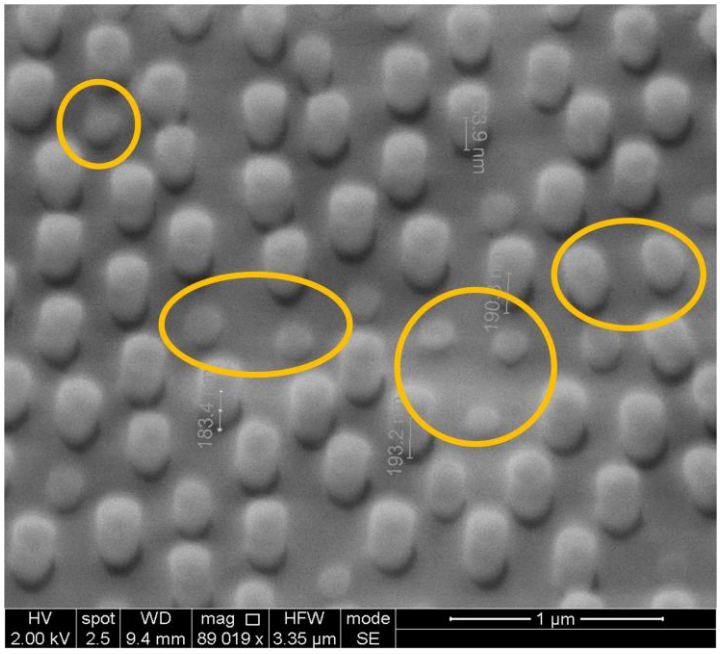

IMAGE 5. SEM IMAGE OF POLYMERIC NANOPILLARS. IN YELLOW CIRCLES, NANOPILLARS WHERE THE POLYMER DID NOT ENTERED INSIDE THE NANOHOLES OF THE PDMS. SCALE = 1 µm.

Therefore, vacuum time was increased up to 1 minute (in pulses of 5 seconds) plus 30 seconds for the samples #1. The quality of the replicas improved: the polymer penetrated into the PDMS nanoholes and a quite homogeneous distribution of nanopillar heights were obtained, but only for EPO-TEK® OG142-87 (Images 9 - 10 and Annex Images 11 - 12). For EPO-TEK® OG603, vacuum time is increased up to 2 minutes (in pulses of 10 seconds) plus 1 minute (in pulses of 30 seconds), but the polymer did not penetrated into the nanoholes (Annex Images 13 - 14).

For the samples #2, although the nanopillars have a bigger diameter (150 and 200 nm), vacuum time was increased in order to achieve a uniform matrix of nanopillars. The time used was 2 minutes (in pulses of 10 seconds) plus 1 minute (in pulses of 30 seconds). With these conditions, an almost perfect penetration of the polymer was achieved in the samples of 200 nm of diameter (images 11-14 and Annex images 15-16 and a quite correct penetration for the 150 nm diameter sample (Annex images 17 - 18).

For the samples #3, vacuum time was also increased, because it is important to achieve the same penetration as the samples #2, but in this case the diameters are smaller (138 and 133 nm). For that reason, 3 minutes (in pulses of 5 seconds) plus 1 minute and 30 seconds (in pulses of 15 seconds) of vacuum was used for both polymers, but it was not possible to fabricate a good replica. Finally, 6 minutes (in pulses of 10 seconds) plus 3 minutes (in pulses of 30 seconds) of vacuum was tried in an attempt to fill completely all the holes , but similar results were obtained.

It has to be said that the time of vacuum of the steps can be changed. The most important thing is to avoid that the polymer starts to boil (or to form "uncontrolled" bubbles). If it happens, the properties of the polymer can be altered , microbubbles can be created within the polymer or big bubbles can remove the polymer from the nanoholes.

PUTTING AND PRESSURING THE GLASS

Once the polymer has penetrated inside the nanoholes of the PDMS mould, a glass has to be put on top to cure the polymer with UV light and to stick it to the glass surface. Such glass surface can be an ordinary microscope slide which has been cleaned before with piranha solution (15 mL of H_2O_2 and 45 mL of H_2SO_4).

This is another crucial step in our replication protocol. We have observed that eliminating the gas was not enough to make the polymer penetrate inside the nanoholes with smaller diameter, so we decided to apply a pressure on the glass to force the polymer to penetrate inside the holes. Furthermore, the weight has to be uniformly distributed through the entire sample. For that reason, a flat weight has to be used. Another strategy can be putting a thick glass and PDMS between the sample and the weight (see figure 6).

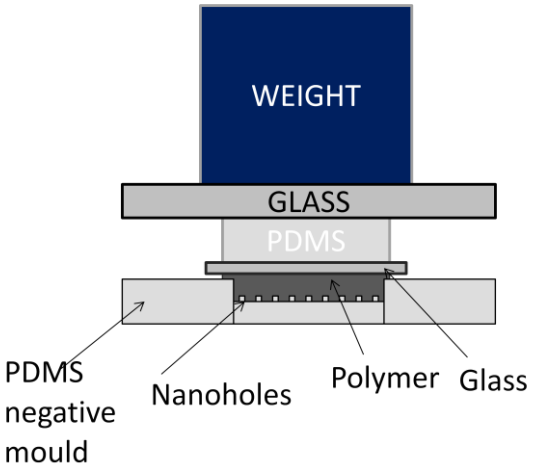

FIGURE 6. REPRESENTATION OF THE STRATEGY TO DISTRIBUTE THE PRESSURE UNIFORMLY

Firstly, we tried to apply the pressure done only by the glass for 20 minutes, but it was not useful, because the glass did not apply enough pressure to help the polymer to enter inside the nanoholes, so any nanopillar was replicated. In the next try we waited for 30 minutes until putting the glass and a weight of 640g, and we kept the pressure on the PDMS for 1 hour and 30 minutes. After a few more tries, it was proved that the first 30 minutes wait without pressure was unnecessary. Therefore, we compared the results applying pressure for 1 hour and 30 minutes, 2 hours and 24 hours. The results were clear: there is an improvement of the penetration between 1 hour 30 minutes and 2 hours, but there were not many differences between 2 hours and 24.

Therefore, we can conclude that immediately after making the vacuum the PDMS mould with polymer has to be covered by the glass and pressured uniformly with a weight for at least 2 hours. Doing this, the polymer will be forced to enter inside the holes.

UV CURING

The recommended cure at a wavelength of 240-365 nm with a power of 100mW/cm for photopolymer EPO-TEK® OG142-87 is more than 2 minutes, while for EPO-TEK® OG603 is more than 5 seconds. However, it has to be taken into account that there is the glass between the UV light and the polymer, and also that the power of the UV lamp used in this work is 80mW at 365 nm, so the curing time will be higher than the recommended.

The proposed curing for EPO-TEK® OG142-87 was exposing for 30 seconds, and waiting for 1 minute until a next exposure of 4 minutes. The first 30 seconds are useful to start to solidify the polymer for doing the first check avoiding moving the glass, which could dirty or damage the replication. Then, the exposure of 4 minutes is the necessary to entirely cure the polymer. Less than 4 minutes is not enough, and more than 4 minutes will overcure the polymer, turning its clear colour to a yellowish one. These times were not changed during all the experiments.

For EPO-TEK® OG603, the initial curing time was 15 seconds of UV exposure, 1 minute of rest and 2 minutes more of UV exposure. After doing some experiments, it was concluded that the time of exposure was not enough: the polymer was cured, but the nanopillars were not strong enough to be straight after removing them from the mould. For that reason, the time was increased up to 15 seconds of UV exposure + 1 minute of rest + 4 minutes more of UV exposure.

THERMAL POST-CURING

From the information of the data sheet, temperature helps EPO-TEK® OG142-87 polymer to be completely cured. The first experiments were carried out without this step, and the results were bad, because the nanopillars buckled and collapsed when they were removed from its mould (Image 6).

Therefore, thermal curing helps the polymer to be harder, but there is another fact that helps to obtain a good replication: the expansion coefficient of PDMS is high, so the nanoholes become smaller with high temperature. In this process, the PDMS push and compact the polymer nanopillars, making easier to remove them from the negative mould when the PDMS is cooled to room temperature. It is useful to put a weight on top of the glass, because it will not allow the PDMS to expulse the polymer when it expands, due to temperature.

The recommended curing conditions are 150ºC for 1 hour. However, we realise that curing for 2 hours helps to achieve a better replication, making easier to remove the nanopillars from its mould without falling down them.

Theoretically, thermal curing is not needed for curing EPO-TEK® OG603 polymer. However, after realising the outstanding improvement with thermal curing in the EPO-TEK® OG142-87 polymer, thermal curing was tried also with this polymer, using the same conditions as for EPO-TEK® OG142-87 (150ºC for 2 hours). The improvement in the stability of the nanopillars was similar for both polymers, so it has also been included as a part of the nanopillar replica fabrication protocol.

REMOVING FROM THE PDMS MOULD

Once the sample is cured using UV light and temperature and it is cooled to room temperature, the glass with the nanopillars can be removed from the PDMS negative mould. The glass and PDMS is turned upside down (the PDMS has to be on top). Then, the PDMS is removed in a similar way comparing to the PDMS removing from the silicon samples. The most useful way to do it is by pressing the glass with one hand and removing the PDMS with the other hand (see Image 7).

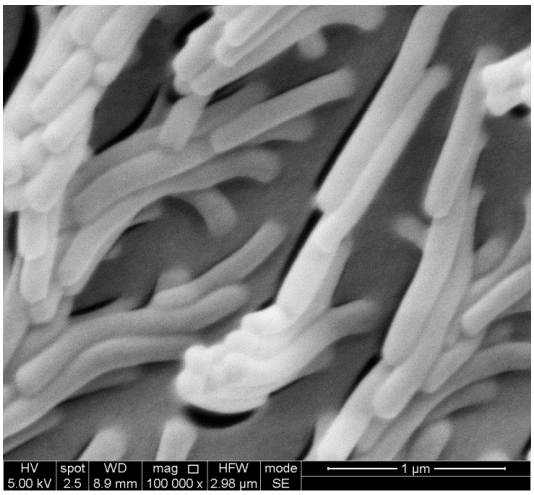

IMAGE 6. SEM IMAGE OF COLLAPSED NANOPILLARS

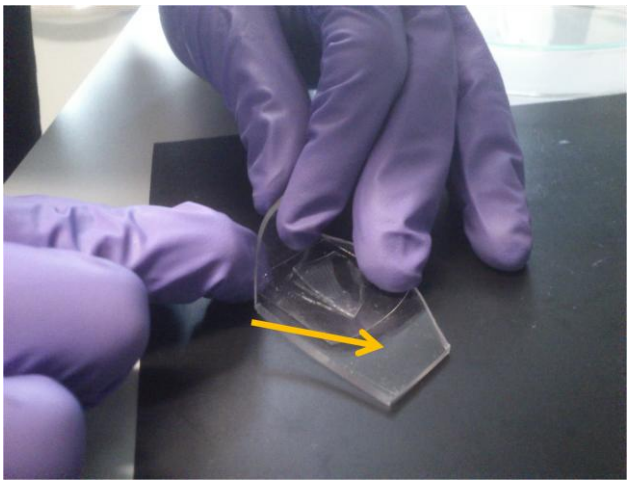

IMAGE 7. REMOVING THE NANOPILLARS FROM THE PDMS MOULD. THE ARROW SHOWS THE DIRECTION OF DEMOLDING

CHECKING

Again, illuminating the sample is a useful and fast way to determine if the replication has succeed or not. As it happens with the negative mould, a regular nanopillar matrix diffract visible light into different wavelengths, depending on the angle of incidence (Image 8). However, seeing bright colours not always means that the replication is correct. The diffraction of light can also be due to an ordered pattern of mistakes or pillar with incorrect height due to improper filling of the PDMS holes. If the sample don't diffract light it means that the polymer have not penetrated at all inside the nanoholes (the sample is transparent) or that the nanopillars have collapsed while were removed from its mould (the sample has white colour).

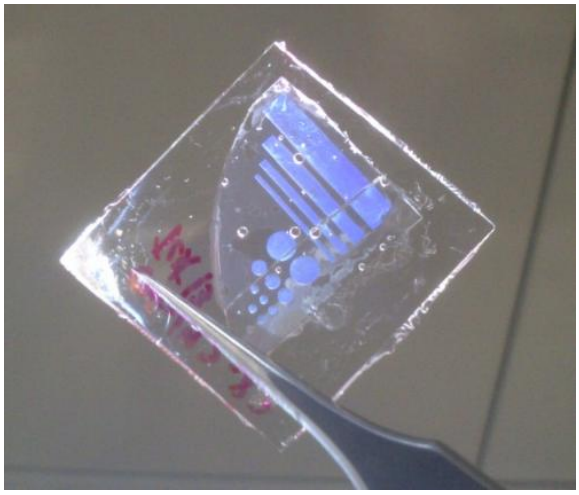

IMAGE 8. LIGHT DIFFRACTION OF THE POLYMERIC NANOPILLARS

GOLD EVAPORATION

Finally, if the replica show diffraction, gold can be evaporated on top, making a layer of 25 nm thick. Since the epoxy polymers are insulators, gold is necessary for looking the nanopillars at Scanning Electron Microscope (SEM). Moreover, the evaporation of gold will also produce plasmonic nanodisks on the nanopillars top, which will produce the LSPR phenomena for the sensing applications.

However, this evaporation can modify the nanopillars. During the evaporation process, there can be a large increase of temperatures, which can affect the nanopillars size. On the other hand, if the evaporation is not vertical, the gold atoms can bend the nanopillars, making harder to determine its size at SEM images.

2.3.3. OPTIMIZED PROTOCOL

In conclusion, the resultant protocols after all the optimization steps is the following:

EPO-TEK® OG142-87

Centrifugation	3000 rpm for 5 minutes
Weight	Depend on the size of the sample (for our samples, 0.25g approximately)
Vacuum	3 minutes (steps of 5s) + 1 minute 30 seconds (steps of 15s)
Putting and pressuring the glass	Glass + PDMS + Bigger glass + 640g Weight on top, for 2 hours
UV Curing	30 seconds UV + 1 minute Without UV + 4 minutes UV
Thermal Curing	150ºC for 2 hours
Removing from the mould and checking by diffraction	
Gold Evaporation	

TABLE 8. OPTIMIZED NANOPILLAR REPLICA PROTOCOL USING EPO-TEK® OG142-87

EPO-TEK® 603

Centrifugation	3000 rpm for 5 minutes
Weight	Depend on the size of the sample (for our samples, 0.20g approximately)
Vacuum	3 minutes (steps of 10s) + 1 minute 30 seconds (steps of 15s)
Putting and pressuring the glass	Glass + PDMS + Bigger glass + 640g Weight on top, for 2 hours
UV Curing	15 seconds UV + 1 minute Without UV + 4 minutes UV
Thermal Curing	150ºC for 2 hours
Removing from the mould and checking by diffraction	
Gold Evaporation	

TABLE 9. OPTIMIZED NANOPILLAR REPLICA PROTOCOL USING EPO-TEK® OG603

2.3.4. RESULTS

Here we show the best replicas achieved with the described protocol. There are several aspects which have to be considered while observing the SEM images of the nanopillar replication. The first one is if the nanopillars have kept straight during the evaporation. It also has to be taken into account if the polymer has penetrated into all the nanoholes, so there is a hexagonal close-packed arrangement and there are not nanopillars missing. It has to be determined if there is a homogeneous distribution of heights. The quantitative determination of heights is done in the section 3 “Characterization”. Finally, other kinds of errors are considered.

Sample #1.3.

Polymer: EPO-TEK® OG142-87

Silicon Master Details	**Diameter:**	151 ± 14 nm
	Height:	928 ± 56 nm
	Separation:	400 nm

TABLE 10. NANOPILLARS DETAILS OF THE SILICON MASTER SAMPLE #1.3

Replication Procedure	**Centrifugation**	3000 rpm for 5 minutes
	Weight	0.30g
	Vacuum	1 minute (pulses of 5 seconds) + 30 seconds
	Pressuring the glass	Glass + 640g Weight for 2 hours
	UV Curing	30 seconds UV + 1 minute WUV + 4 minutes UV
	Thermal Curing	150ºC for 1 hour

TABLE 11. PROTOCOL USED FOR THE REPLICATION OF SAMPLE #1.3 WITH EPO-TEK® OG142-87

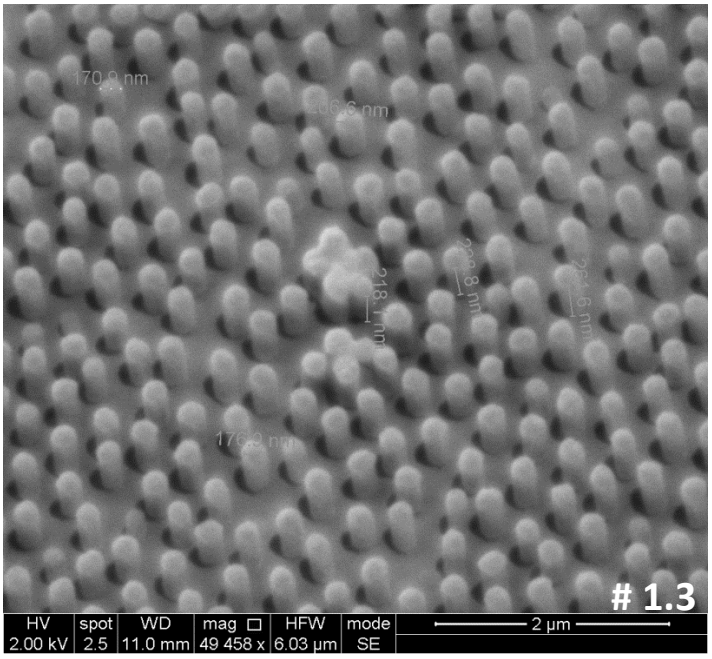

IMAGE 9. SEM IMAGE OF THE REPLICATION OF SAMPLE #1.3 USING EPO-TEK® OG142-87. SCALE = 2 µm

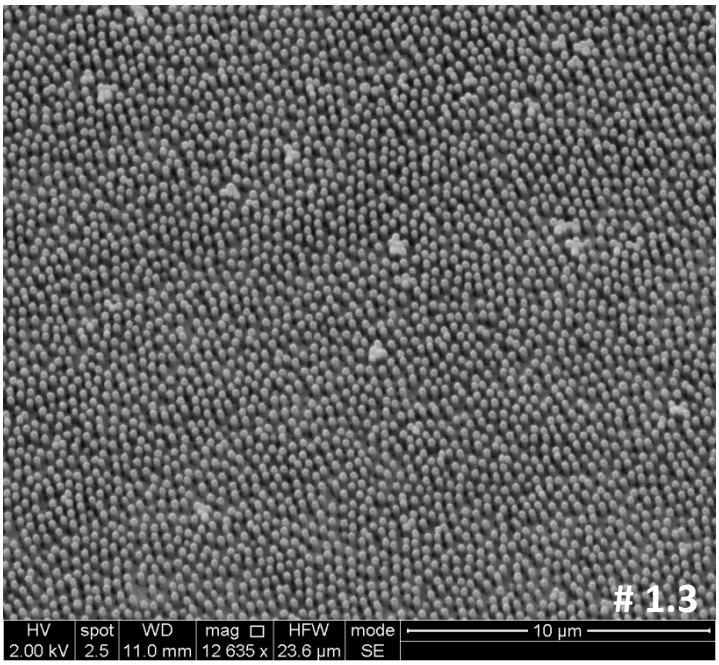

IMAGE 10. SEM IMAGE OF THE REPLICATION OF SAMPLE #1.3 USING EPO-TEK® OG142-87. SCALE = 10 µm

It can be seen that there has been an homogeneous penetration of the polymer inside the nanoholes in all the sample (Image 9). If we take a deeper look on the images, there are some nanopillars which are a little bit smaller than the others. Since it is very difficult to obtain a matrix of perfect nanopillars without a single mistake, the ratio between mistakes and well-replicated nanopillars has to be considered. In this case this ratio is quite small (Image 10). On the other hand, the nanopillars are slightly bent in the same direction. Our hypothesis is that the nanopillars have bent during the gold evaporation due to the oblique incidence of the gold atoms. Finally, there are some nanopillars which are stuck together. These punctual mistakes could appear due to an error in the silicon master. The same conclusions can be extrapolated for the replication of samples #1.1 and #1.2 (Annex Images 11-12).

Sample #2.2:

Polymer: EPO-TEK® OG142-87

Silicon Master Details	**Diameter:**	194 ± 12 nm
	Height:	803 ± 50 nm
	Separation:	400 nm

TABLE 12. NANOPILLARS DETAILS OF THE SILICON MASTER SAMPLE #2.2

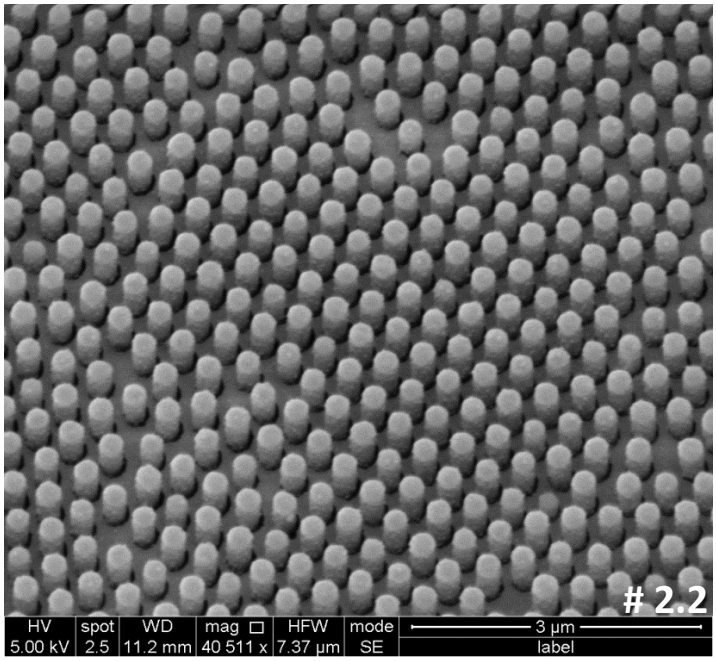

IMAGE 11. SEM IMAGE OF THE REPLICATION OF SAMPLE #2.2 USING EPO-TEK® OG142-87. SCALE = 3 µM

Replication Procedure	**Centrifugation**	3000 rpm for 5 minutes
	Weight	0.42g
	Vacuum	2 minutes (pulses of 10 seconds) + 1 minute (pulses of 30 seconds)
	Pressuring the glass	Glass + 640g Weight for 2 hours
	UV Curing	30 seconds UV+ 1 minute WUV+ 4 minutes UV
	Thermal Curing	150ºC for 1 hour

TABLE 13. PROTOCOL USED FOR THE REPLICATION OF SAMPLE #2.2 WITH EPO-TEK® OG142-87

These replications were successful. It is clear that the nanopillars are straight, except for the replication #2.3 (Annex Image 16), where nanopillars are long, so it is easier that the nanopillars will be bent. There is an homogeneous distribution of heights and there are not nanopillars missing (they are in an hexagonal close-packed arrangement). These images can be used as a model of how the nanopillar replica must be.

It is important to mention that the difference of diameter (150 nm for samples #1, 200 nm for samples #2) indicates the difficulty of the replication. With this replication procedure, nanopillars with diameter of 200 nm with an aspect ratio of 1:8 can be replicated without problems.

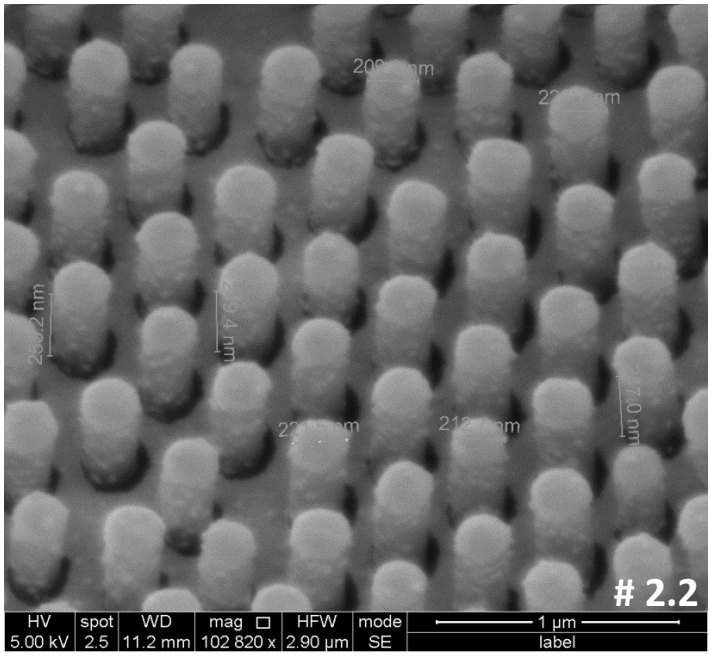

IMAGE 12. SEM IMAGE OF THE REPLICATION OF SAMPLE #2.2 USING EPO-TEK® OG142-87. SCALE = 1 µm

Sample #2.2:

Polymer: EPO-TEK® OG603

Silicon Master Details	**Diameter:**	194 ± 12 nm
	Height:	803 ± 50 nm
	Separation:	400 nm

TABLE 14. NANOPILLARS DETAILS OF THE SILICON MASTER SAMPLE #2.2

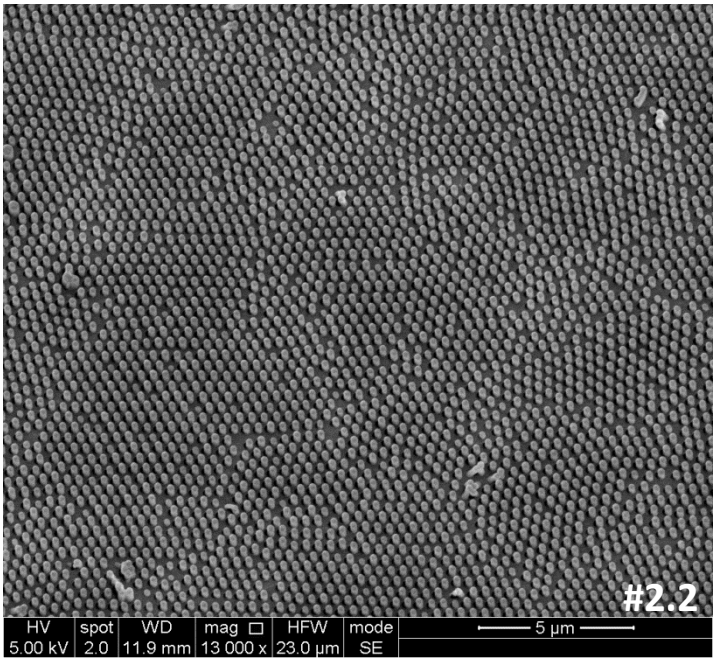

IMAGE 13. SEM IMAGE OF THE REPLICATION OF SAMPLE #2.2 USING EPO-TEK® OG603. SCALE = 5 µM

Replication Procedure	**Centrifugation**	3000 rpm for 5 minutes
	Weight	0.30g
	Vacuum	3 minutes (pulses of 10 seconds) + 1 minute 30 seconds (pulses of 30 seconds)
	Pressuring the glass	Glass + 640g Weight for 2 hours
	UV Curing	30 seconds UV+ 1 minute WUV+ 3 minutes UV
	Thermal Curing	WITHOUT THERMAL CURING

TABLE 15. PROTOCOL USED FOR THE REPLICATION OF SAMPLE #2.2 WITH EPO-TEK® OG603

The replication of the same silicon master using EPO-TEK® OG603 polymer has also been successful. On the one hand, nanopillars are quite homogeneous and there are not large areas without nanopillars. However, it can be seen on Annex Image 20 the importance of thermal curing. With this protocol, it is expected to achieve perfect nanopillars while replicating nanopillars of 200 nm of diameter and 449 nm of height, but in this case some of them have fallen when the PDMS mould was removed. Therefore, without thermal curing the removing of the nanopillars from its mould has to be extremely delicate.

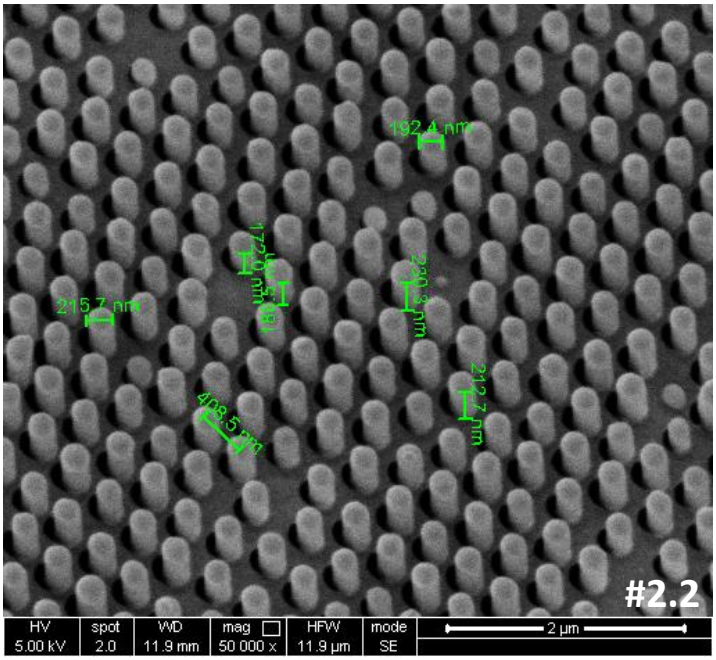

IMAGE 14. SEM IMAGE OF THE REPLICATION OF SAMPLE #2.2 USING EPO-TEK® OG603. SCALE = 2 µM

The replication of the silicon samples #3 has been not fully successful. There are areas without nanopillars, and taking a deeper look it is clear that the nanopillar heights are not equal. In addition, there are some fallen nanopillars. The replication using EPO-TEK® OG142-87 (images 17-18) has been better than EPO-TEK® OG603 (images 15-16), maybe because the vacuum time has been doubled. Since this tendency has been followed in all the samples, it is concluded that is more difficult to replicate nanopillars with EPO-TEK® OG603 than with EPO-TEK® OG142-87, but there are not large differences between them.

Sample #3.1

Polymer: EPO-TEK® OG603

Silicon Master Details	**Diameter:**	138 ± 8 nm
	Height:	489 ± 24 nm
	Separation:	400 nm

TABLE 16. NANOPILLARS DETAILS OF THE SILICON MASTER SAMPLE #3.1

Replication Procedure	**Centri-fugation**	3000 rpm for 5 minutes
	Weight	0.20g (#3.1) 0.23g (#3.2)
	Vacuum	3 min (pulses of 10 s) + 1 min 30 s (pulses of 30 s)
	Pressuring the glass	Glass + Big glass + 640g Weight for 2 hours
	UV Curing	15 s UV + 1 min WUV + 4 min UV
	Thermal Curing	150ºC for 2 hours

TABLE 17. PROTOCOL USED FOR THE REPLICATION OF SAMPLE #3.1 WITH EPO-TEK® OG603

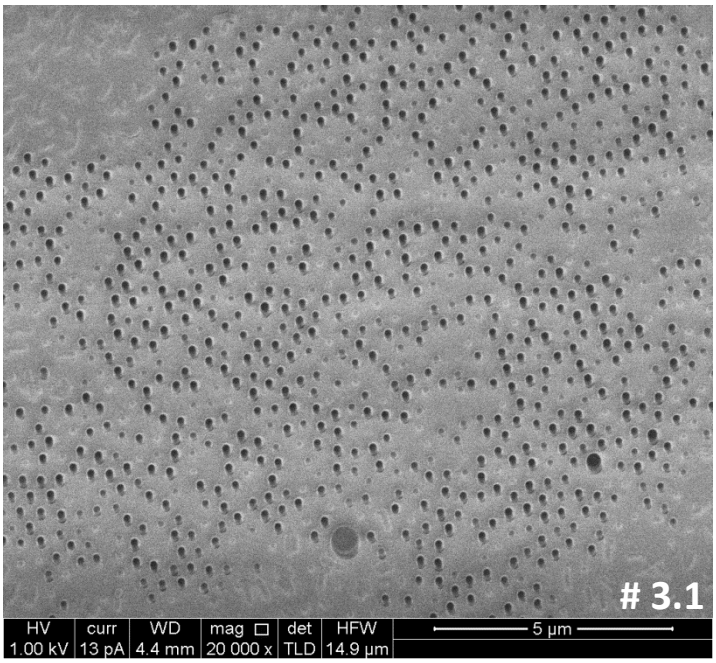

IMAGE 15. SEM IMAGE OF THE REPLICATION OF SAMPLE #3.1 USING EPO-TEK® OG603. SCALE = 5 µM

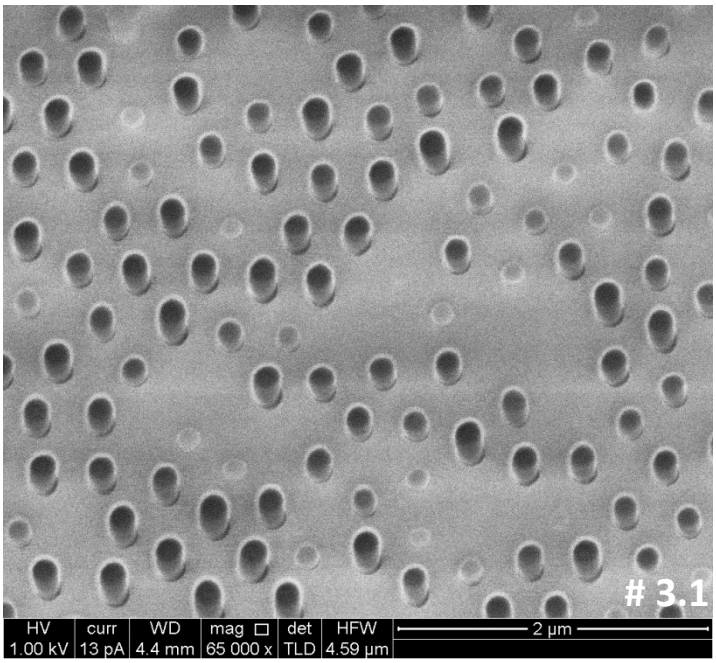

IMAGE 16. SEM IMAGE OF THE REPLICATION OF SAMPLE #2.2 USING EPO-TEK® OG603. SCALE = 2 µm

Sample #3.2

Polymer: EPO-TEK® OG142-87

Silicon Master Details	**Diameter:**	133 ± 13 nm
	Height:	976 ± 50 nm
	Separation:	400 nm

TABLE 18. NANOPILLARS DETAILS OF THE SILICON MASTER SAMPLE #3.2

Replication Procedure	**Centri-fugation**	3000 rpm for 5 minutes
	Weight	0.25g (#3.1) 0.23g (#3.2)
	Vacuum	6 min (pulses of 10 s) + 3 min (pulses of 30 s)
	Pressuring the glass	Glass + Big glass + 640g Weight for 2 hours
	UV Curing	30 s UV + 1 min WUV + 4 min UV
	Thermal Curing	150ºC for 2 hours

TABLE 19. PROTOCOL USED FOR THE REPLICATION OF SAMPLE #3.2 WITH EPO-TEK® OG142-87

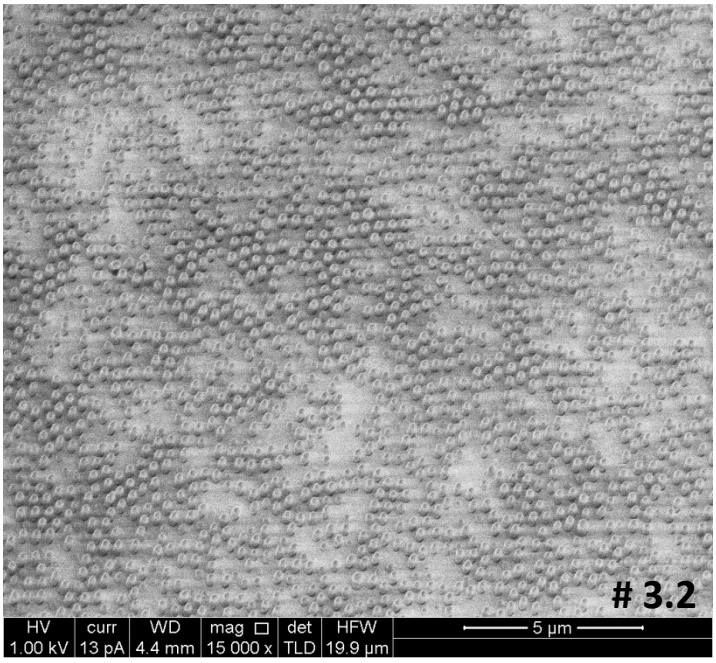

IMAGE 17. SEM IMAGE OF THE REPLICATION OF SAMPLE #3.2 USING EPO-TEK® OG142-87. SCALE = 5 µM

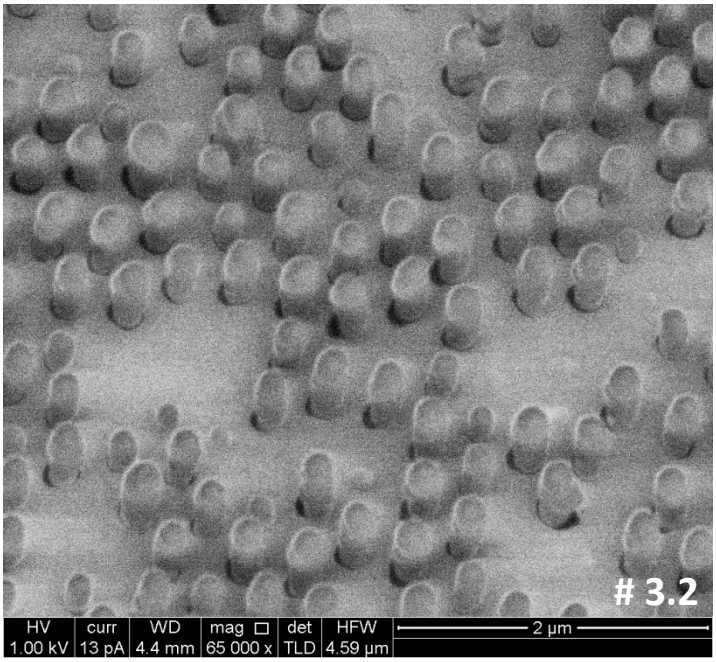

IMAGE 18. SEM IMAGE OF THE REPLICATION OF SAMPLE #3.2 USING EPO-TEK® OG603. SCALE = 2 µm

In conclusion, we have observed that the diameter of the nanoholes in the PDMS mould plays a crucial role in the quality of the replicas. With our protocol, the replicas of nanopillars with diameters in the order of 200 nm and above is barely perfect. For diameters ranging from 200 and 150 the replications have a good quality, but some defects start to appear. In contrast, the replica of nanopillar with diameter below 150 nm becomes much more complicated. However, it could be possible in the future to improve and make drastic changes to this protocol to be able to replicate nanopillars with this size. Not being able to replicate this size of nanopillars is not an important problem because polymeric nanopillars with diameters between 150 and 180 nm and different aspect ratios are suitable for the biomimetic nano-opto-elastic biosensor, which is presented here.

3. CHARACTERIZATION

3.1. ELASTIC CONSTANT

As it has been explained before, knowing the dimensions of the polymeric nanopillars will allow to calculate their spring constant, and therefore their effective Young modulus. Depending on which spring constant they have, the array of nanopillars will mimic a different biological tissue (see table 1). Therefore, here we present the effective Young modulus of the best nanopillar replicas and their correlation with a biological tissue. These results will give an idea of what range of tissues can be mimicked with this protocol of nanopillar replication.

The dimensions (diameter and height) which are presented here are the average of the measurements extracted from the SEM images presented in this work, and they follow a gaussian distribution (histograms shown in Annex 3). The elastic constant is calculated using the equation 1 and the effective Young modulus (E_{eff}) is found using the equation 2. These values has only been calculated for the samples which have been well-replicated.

3.1.1. RESULTS AND DISCUSSION

Polymer	Sample	Silicon nanopillar details (nm)	Polymeric nanopillar replica details (nm)	Elastic constant (N/m)	Effective Young modulus (MPa)
EPO-TEK® OG142-87	#1.3	Diameter =151 ± 14	Diameter = 178 ± 17	0,2 ± 0,14	1,6 ± 1,1
		Height =928 ± 56	Height =1091 ± 207		
	#2.1	Diameter =197 ± 15	Diameter = 197 ± 21	4,45 ± 4,28	3,2 ± 3,1
		Height =592 ± 67	Height = 443 ± 97		
	#2.2	Diameter =194 ± 12	Diameter = 222 ± 16	0,53 ± 0,15	3,5 ± 2,9
		Height =803 ± 50	Height = 1050 ± 286		
EPO-TEK® OG603	#2.1	Diameter =194 ± 12	Diameter = 198 ± 25	3,1 ± 2,6	2,3 ± 1,9
		Height =803 ± 50	Height = 501 ± 115		
	#2.2	Diameter =194 ± 12	Diameter = 188 ± 17	0,98 ± 0,49	7,4 ± 3,8
		Height =803 ± 50	Height = 689 ± 79		

TABLE 20. COMPARATIVE TABLE OF THE NANOPILLARS MASTER NANOPILLARS AND THEIR REPLICATION, WITH THEIR CORRESPONDENT ELASTIC CONSTANT AND EFFECTIVE YOUNG MODULUS

Comparing the dimensions between silicon and polymeric nanopillars, there are some aspects which has to be mentioned: the diameters of the replicas are the same as the silicon master. Regarding the heights, the height of the replicated nanopillars are smaller than in the silicon. The differences between both heights is a good indicator of the quality of the replication because it tells how much the polymer has penetrated into the nanoholes of the PDMS mould. Therefore, it is clear that it is difficult to obtain a perfect replication with the polymer EPO-TEK® OG603.

It is important to mention that this behaviour did not happened for the samples #1.3 and #2.2 (EPO-TEK® OG142-87), where the diameters and the heights of the replication are bigger than in the silicon. It can occur for different reasons: during the evaporation process, the sample is heated making the nanopillars to expand. Moreover, the gold can fall not vertically, making the nanopillars to bend, causing errors in the measurements. Furthermore, gold can be accumulated on the top of the nanopillar, forming a nanodisk with an effective diameter which is bigger than the nanopillar. Finally, it is also important to consider that the SEM images of silicon and polymeric nanopillars do not show the same nanopillars.

Regarding the elastic constant and the effective Young modulus, we have achieved the fabrication of polymeric nanopillar arrays, with an effective Young modulus from 1,6 to 7,4 MPa. These stiffnesses correspond to the bone tissue, and the minimum Young modulus of 1,6 MPa is quite close to mime cartilaginous tissue.

It is noticeable that the standard deviation of the effective Young modulus is large, as well as for the elastic constant. It has to be considered that most part of the errors in the diameter and height of the nanopillar replication comes from the errors of the silicon mould. When the elastic constant is calculated, these errors are increased, due to the propagation of uncertainty rules[24]. However, these large uncertainties are not a problem for the conclusions of this work. What is important to know is the order of magnitude of the effective Young modulus of the polymeric nanopillars which it is possible to replicate with the described protocol.

3.2. CONTACT ANGLE

It is important to know how hydrophobic the surface with polymer nanopillars is because when they will be put into a microfluidic system, the aqueous solutions have to move between the nanopillars, so an hydrophilic surface is needed.

Contact angle measurements is a useful way to do determine the hydrophobicity of our samples. These measurements has been carried out using *Kruss EasyDrop* and the software *Drop Shape Analysis*. A single water drop is put on the surface of the sample. It is registered by a camera and the software adjust the shape of the drop to obtain the contact angle.

It also has to be taken into account that the nanopillars will have gold nanodisks on top, which is the strategy to use the nanopillar array not only as a biomimetic platform but also as a LSPR sensor.

3.2.1. RESULTS AND DISCUSSION

Contact angle of several samples of different diameters and heights were measured. These are the results:

Height (nm)	Diameter (nm)	Contact angle (degrees)
800	186	130,7 ± 0,15
500	158	126.3 ± 0.24
940	150	131.7 ± 0.18
449	200	129.8 ± 0.16
735	200	135.2 ± 0.18
1478	200	140.4 ± 0.05
1079	150	141.4 ± 0.15

TABLE 21. CONTACT ANGLE MEASUREMENTS OF DIFFERENT SAMPLES OF POLYMERIC NANOPILLARS

These results confirm the initial hypothesis: nanopillars with gold evaporated on top are hydrophobic, all the samples has a similar contact angle, no matter what are their dimensions. For that reason, it is proposed that an oxygen plasma would be a solution to make this nanopillars more hydrophilic.

Therefore, an oxygen plasma of 50W, 45% of air flow, during 30 seconds is done to the nanopillar samples and the contact angle is measured afterwards. These are the results:

Height (nm)	Diameter (nm)	Contact angle (degrees)
800	186	13.1 ± 3.80
500	158	9.2 ± 0.35
940	150	23.2 ± 1.89
449	200	14.2 ± 0.83
735	200	15.1 ±0.31
1478	200	15.2 ± 1.23
1079	150	28.1 ± 3.66

TABLE 22. CONTACT ANGLE MEASUREMENTS OF DIFFERENT SAMPLES OF POLYMERIC NANOPILLARS AFTER AN OXYGEN PLASMA

It is clear that the oxygen plasma reduce drastically the contact angle making the nanopillars more hydrophilic. The oxygen plasma turn the nanopillar surface into an hydrophilic one. Therefore, an oxygen plasma will help the nanopillar structure in further microfluidic experiments. It will be necessary to demonstrate in the future how long the nanopillars remain hydrophilic after the oxygen plasma is done.

4. LSPR

The nano-opto-elastic sensor proposed in this work will follow the interaction between the array of nanopillars and cells by Localized Surface Plasmon Resonance (LSPR) of the nanoplasmonics caps.

As it has been explained before, this interaction will be possible after the functionalization of nanopillars with amino acid sequences from proteins of the extracellular matrix. Two complementary peptides are used: the first one is bound to the gold surface by a thiol group of a cysteine. The second is complementary to the former, with and added bioactive cell recognition sequence from an extracellular matrix protein (such as fibronectin or integrin). Since they are complementary

due to electrostatic interactions, their binding can be broken by a pH change. Therefore, complementary peptides with different recognition sequences of amino acids such as RGD, PHSRN, DGEA or YIGSR can be used, converting this system into reversible (Figure 7).

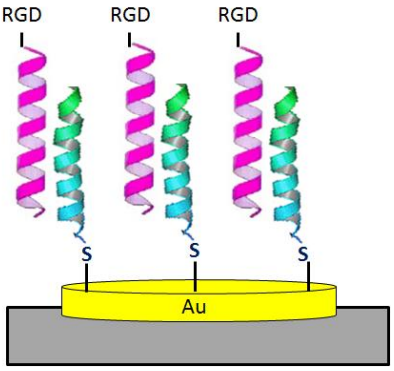

FIGURE 7. FUNCTIONALIZED GOLD NANODISK USING 2 COMPLEMENTARY PEPTIDES. RGD SEQUENCE (ARG-GLY-ASP) IS ADDED TO THE SECOND PEPTIDE

However, it is important to know about this optical method of detection before using it with the samples of polymeric nanopillars. Therefore, here are presented the first approaches using this sensor, by using a surface with gold nanodisks, functionalized with two complementary peptides: ECV and KV (data sheet in Annex 4). The aim of these experiments is to find the dissociation constant between both peptides when ECV is anchored to the surface and determine if this pair of peptides would be useful for the forthcoming nano-opto-elastic sensor.

4.1. EXPERIMENTAL SETUP

Firstly, gold nanodisks must be functionalized with ECV peptide. The surface of gold nanodisks is fabricated by colloidal lithography[14]. To functionalized the nanodisks with the ECV peptide, 200µL of 108 µM solution is incubated overnight on top of the gold nanodisks surface. After that, this surface is placed in the LSPR system (Image 19). It consists on a Teflon flow cell, where the nanodisk surface is situated, with a prism which focuses the white light to the gold nanodisk surface. The samples with peptides are flowed through the flow cell using a fluidic system which consist on a pump, used to maintain a continuous flux of phosphate buffer saline solution (PBS) of 10 mM, and an injection valve, which will be used to inject the desired solutions in the system (in this case, peptide KV solutions). The reflected light is collected by an spectrophotometer and the data is displayed using a homemade software, which acquires real-time data on the variation of the reflected wavelength.

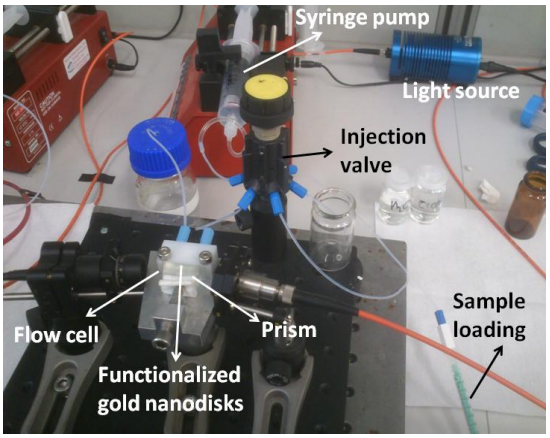

IMAGE 19. EXPERIMENTAL SETUP FOR LSPR MEASUREMENTS

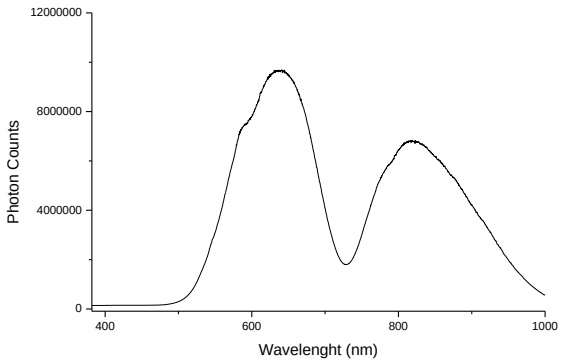

FIGURE 8. REFLECTED WHITE LIGHT SPECTRUM. THE MINIMUM CORRESPONDS TO THE WAVELENGTH WHERE THE LSPR OCCURS.

The spectrum of the reflected light shows a minimum at the wavelength in which the LSPR occurs (Figure 8). This critical wavelength varies depending on the local refractive index, so its changes are followed for obtaining information on the binding of the complementary peptide to the functionalized gold nanodisks.

4.2. RESULTS AND DISCUSSION

KV peptide solutions of different concentrations are passed through the flow cell. The local binding between the complementary peptides produces a displacement on the LSPR peak. Measuring this displacement for different concentrations it is possible to obtain the dissociation constant between both peptides. 1mM chlorhydric acid solution (pH = 3) is passed after every measurement to broke the interaction between both peptides.

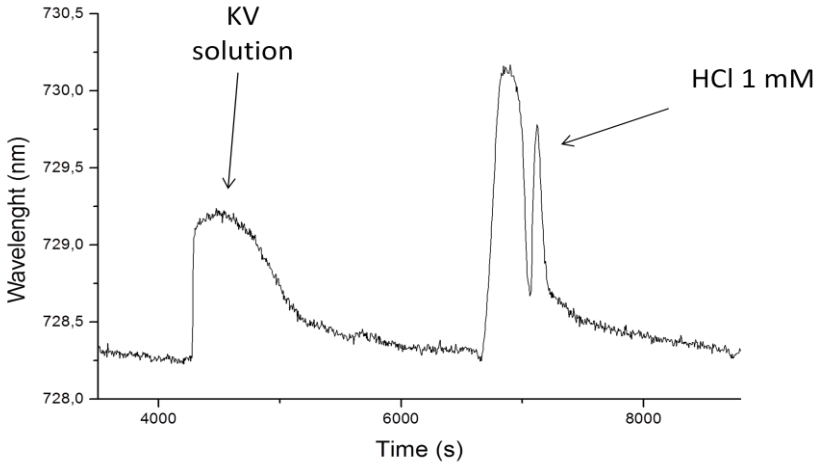

FIGURE 9. CRITICAL WAVELENGTH PLOT VS TIME. THE FIRST PEAK CORRESPOND TO THE KV PEPTIDE SOLUTION. THE SECOND ONE CORRESPOND TO A 1MM HCL SOLUTION.

DISSOCIATION CONSTANT CALCULUS

Taking the values of the dissociation constant of the data sheet as a reference, taking into account that this value will be higher because one peptide is anchored to the surface, the concentrations which are used to find the dissociation constant will be between 1 µM and 90 µM. The results are shown in Figure 10.

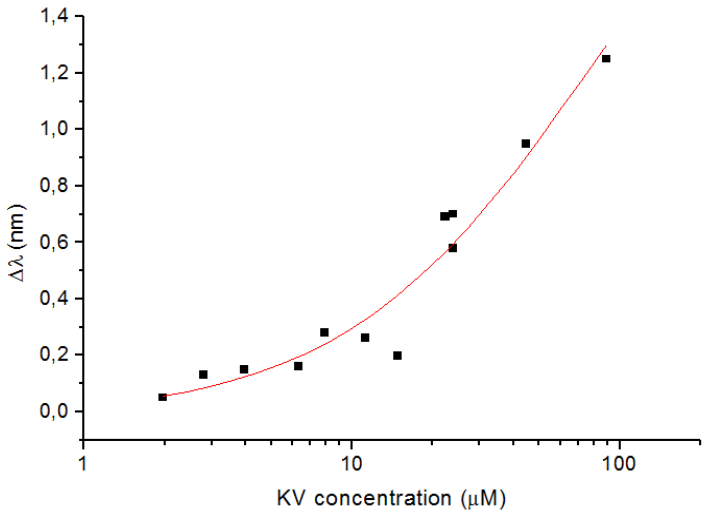

FIGURE 10. PLOT OF THE CRITICAL WAVELENGTH VARIATION VS CONCENTRATION OF COMPLEMENTARY PEPTIDE. A SIGMOIDAL FUNCTION (IN RED) IS ADJUSTED TO THE EXPERIMENTAL POINTS

DISCUSSION

The presented affinity plot is fitted to a sigmoidal function and the turning point of the function correspond to the dissociation constant. However, here is not presented the value of the dissociation constant because, in these measurements, the sigmoidal curve has not been found completely (the upper plateau is not shown).

There is a clear conclusion with this results: the interaction between both peptides has to be strong enough to hold up the binding of cells, as well as other processes. Values of the dissociation constant below 1 µM would be suitable for the nano-opto-elastic sensor. However, the dissociation constant of this pair of peptides is larger than 30 µM, so they will be not useful for the functionalization of nano-opto-elastic sensors.

Therefore, it will be necessary to use a pair of complementary peptides with higher affinity, such as a larger chain of amino acids, or with different configurations[25].

5. MICROFLUIDICS

One of the most important advantages about the proposed nano-opto-elastic sensor is that the system of polymeric nanopillar arrays can be directly integrated into a microfluidic channel, replicating the nanopillars and the channel at the same time.

Using this strategy, the replica will form a mechanically stable monolithic structure. Here is presented the first design of this microfluidic channel, as well as the whole system.

5.1. MICROFLUIDICS DESIGN

A bone-shaped microfluidic channel will be used. This channel will contain the polymeric nanopillars in the middle, integrated in the same structure. Both ends will be the entrance and the exit of the solutions. This polymeric channel will be covered by a PDMS layer to seal the microchannel an enable the liquid flow without leakages. There will be two holes in the PDMS, where the tubes will be placed to introduce the different solutions into the system (see Figure 11).

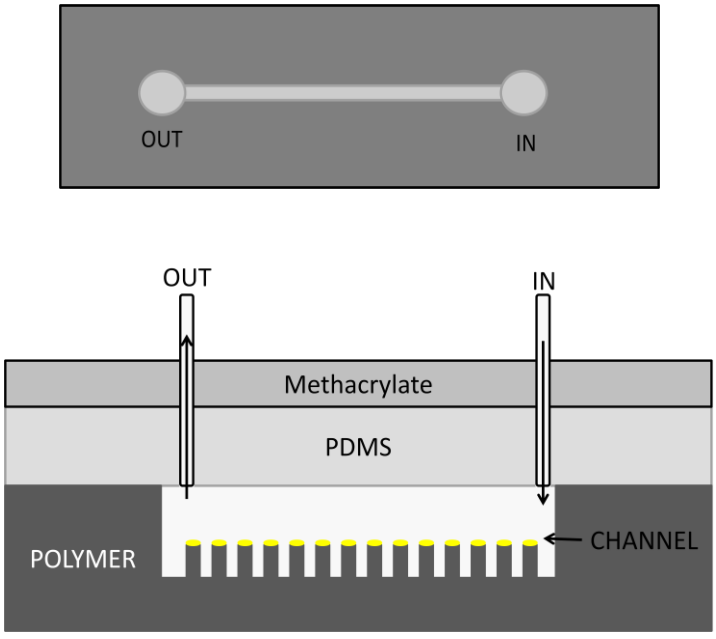

FIGURE 11. SCHEMATIC REPRESENTATION OF THE FIRST MICROFLUIDIC CHANNEL DESIGN

6. CONCLUSIONS

The main conclusions of this project are the following:

- The fabrication protocol of polymeric nanopillar arrays has been optimized. Furthermore, the difficulties that imply the reduction of diameter of nanopillars has been demonstrated. It has been proved that with this protocol the dimension limits where nanopillars can be well-replicated is a diameter of 150 nm with an aspect ratio of 1:6.
- The best nanopillar replications have been characterized by SEM and contact angle measurements. On the one hand, SEM images show that a quite homogeneous distribution of nanopillar diameters and heights are achieved, but it can be improved. Moreover, using two different photocurable polymers nanopillar arrays with effective Young modulus between 1,6 and 7,4 MPa has been fabricated, which mimic bone tissue and almost cartilaginous tissue. On the other hand, oxygen plasma is required to convert the nanopillars into an hydrophilic surface, enabling the proper flow of the solutions through the nanopillar array.
- Using a LSPR sensor, it has been proved that the presented peptides (ECV and KV) are not useful for the functionalization of gold nanodisks since they have very low affinity for this application.
- Finally, the first design of the microfluidic system is presented.

7. FUTURE PERSPECTIVES

This work is only a little part of a large project related to the development of the biomimetic nano-opto-elastic sensor, which has been presented at the introduction. For that reason, more work has to be done to make the proposed biosensor become a reality. Regarding the aspects of the project considered in this work, the future aims are the following:

- Reducing the effective Young modulus: It is important to be able to mime all kind of tissues with this array of polymeric nanopillars. Therefore, the effective Young modulus should reduced. Nanopillars with a diameter between 150 and 180 nm are useful for the nano-opto-elastic sensor. Therefore, it has to be determined the maximum aspect ratio which is possible to replicate successfully with this protocol in order to obtain the minimum effective Young modulus. Another possibility is to use polymers with lower Young modulus, which will allow the use of nanopillars with smaller aspect ratios.
- Minimizing the errors in the dimensions: The different effective Young modulus presented in this work had a large standard deviation. This happened because the silicon master fabrication does not fabricate identical nanopillars and these mistakes are enlarged in the replication. For that reason will be necessary to change the fabrication technique of the silicon master into a better one, such as nano-imprint lithography to have a monodisperse array of silicon nanopillars by metal assisted chemical etching.
- Testing how much time the nanopillar surface remain hydrophilic after the oxygen plasma: It is necessary to know it before starting the integration of all the system for assuring the proper flow of the solutions
- Finding a pair of complementary peptides with higher affinity: It has been proved that ECV and KV are not useful because they have low affinity between them. Therefore, it is necessary to find two peptides with higher affinity for the biofunctionalization.
- Following the design of the microfluidic channel and the integration of the whole system.

8. ACKNOWLEDGEMENTS

I would like to thank all the people (family, teachers and friends) who have encouraged me to keep motivated about science and end the nanoscience & nanotechnology degree. Specifically, I would like to thank Borja Sepúlveda for accepting me to work in this project and Iraís Solís for all the help I have received from her, as well as all that she has taught to me. I would also like to thank the NanoB2A group partners for the warm reception I have received. Finally, I would like to thank my lab partners Àngel and Roger for all the good moments in the lab, and my classmate and flatmate Edu for all the scientific discussions about this work and the exasperating days of writing. It was worth it.

9. REFERENCES

1 Geoffrey M. Cooper, R. E. H. The Cell: a Molecular Approach. **5th Edition**, 613-621 (2009).

2 Heilker, R., Wolff, M., Tautermann, C. S. & Bieler, M. G-protein-coupled receptor-focused drug discovery using a target class platform approach. *Drug discovery today* **14**, 231-240 (2009).

3 Kenakin, T. P. Cellular assays as portals to seven-transmembrane receptor-based drug discovery. *Nature Reviews Drug Discovery* **8**, 617-626 (2009).

4 Isherwood, B. *et al.* Live cell in vitro and in vivo imaging applications: accelerating drug discovery. *Pharmaceutics* **3**, 141-170 (2011).

5 Hoffman, B. D., Grashoff, C. & Schwartz, M. A. Dynamic molecular processes mediate cellular mechanotransduction. *Nature* **475**, 316-323 (2011).

6 Janmey, P. A. & Miller, R. T. Mechanisms of mechanical signaling in development and disease. *Journal of cell science* **124**, 9-18 (2011).

7 Wirtz, D., Konstantopoulos, K. & Searson, P. C. The physics of cancer: the role of physical interactions and mechanical forces in metastasis. *Nature Reviews Cancer* **11**, 512-522 (2011).

8 Engler, A. J., Sen, S., Sweeney, H. L. & Discher, D. E. Matrix elasticity directs stem cell lineage specification. *Cell* **126**, 677-689 (2006).

9 Du Roure, O. *et al.* Force mapping in epithelial cell migration. *Proceedings of the National Academy of Sciences of the United States of America* **102**, 2390-2395 (2005).

10 Roos, W., Ulmer, J., Gräter, S., Surrey, T. & Spatz, J. P. Microtubule gliding and cross-linked microtubule networks on micropillar interfaces. *Nano letters* **5**, 2630-2634 (2005).

11 Saez, A., Buguin, A., Silberzan, P. & Ladoux, B. Is the mechanical activity of epithelial cells controlled by deformations or forces? *Biophysical journal* **89**, L52-L54 (2005).

12 Tan, J. L. *et al.* Cells lying on a bed of microneedles: an approach to isolate mechanical force. *Proceedings of the National Academy of Sciences* **100**, 1484-1489 (2003).

13 Ghibaudo, M. *et al.* Traction forces and rigidity sensing regulate cell functions. *Soft Matter* **4**, 1836-1843 (2008).

14 Ortiz, M. A. O. Towards Highly Sensitive and Multiplexed Nanoplasmonic Biosensors. (2012).

15 Becker, B. & Cooper, M. A. A survey of the 2006–2009 quartz crystal microbalance biosensor literature. *Journal of Molecular Recognition* **24**, 754-787 (2011).

16 Vashist, S. K. A review of microcantilevers for sensing applications. *J. of Nanotechnology* **3**, 1-18 (2007).

17 Krupin, O., Asiri, H., Wang, C., Tait, R. N. & Berini, P. Biosensing using straight long-range surface plasmon waveguides. *Optics express* **21**, 698-709 (2013).

18 Jiang, L., Yang, J., Wang, S., Li, B. & Wang, M. Fiber Mach–Zehnder interferometer based on microcavities for high-temperature sensing with high sensitivity. *Optics letters* **36**, 3753-3755 (2011).

19 Barnes, W. L., Dereux, A. & Ebbesen, T. W. Surface plasmon subwavelength optics. *Nature* **424**, 824-830 (2003).

20 Nuzzo, R. G. & Allara, D. L. Adsorption of bifunctional organic disulfides on gold surfaces. *Journal of the American Chemical Society* **105**, 4481-4483 (1983).

21 Lin, S.-Y., Tsai, Y.-T., Chen, C.-C., Lin, C.-M. & Chen, C.-h. Two-step functionalization of neutral and positively charged thiols onto citrate-stabilized Au nanoparticles. *The Journal of Physical Chemistry B* **108**, 2134-2139 (2004).

22 Otte, M. A. *et al.* Improved biosensing capability with novel suspended nanodisks. *The Journal of Physical Chemistry C* **115**, 5344-5351 (2011).

23 Miljkovic, V. D., Pakizeh, T., Sepulveda, B., Johansson, P. & Kall, M. Optical Forces in Plasmonic Nanoparticle Dimers†. *The Journal of Physical Chemistry C* **114**, 7472-7479 (2010).

24 Ku, H. Notes on the use of propagation of error formulas. *Journal of Research of the National Bureau of Standards* **70** (1966).

25 Aili, D. *et al.* Polypeptide folding-mediated tuning of the optical and structural properties of gold nanoparticle assemblies. *Nano letters* **11**, 5564-5573 (2011).

ANNEX

1. SILICON NANOPILLARS (SEM IMAGES):

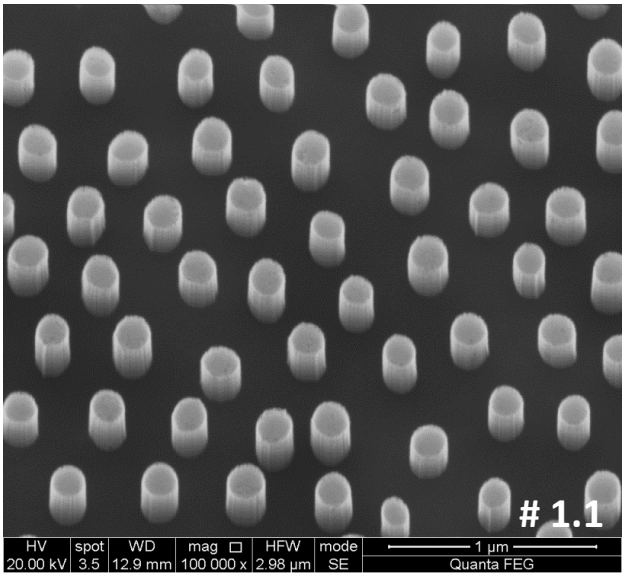

ANNEX IMAGE 1. SEM IMAGE OF SILICON NANOPILLARS (SAMPLE #1.1). SCALE = 1 µm

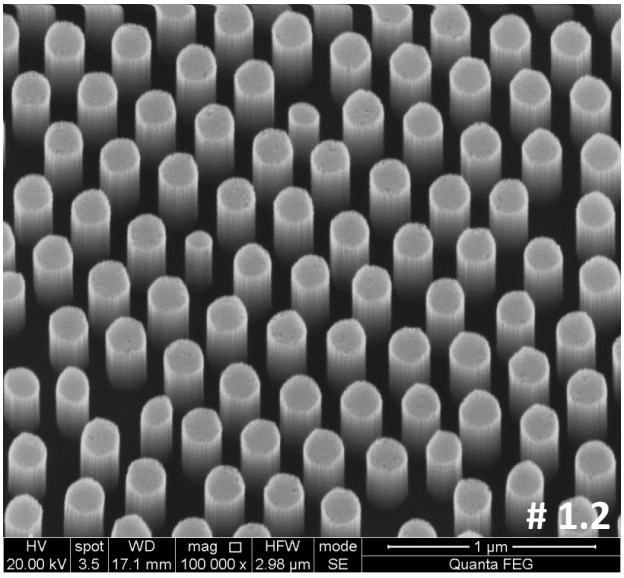

ANNEX IMAGE 2. IMAGE OF SILICON NANOPILLARS (SAMPLE #1.2). SCALE = 1 µm

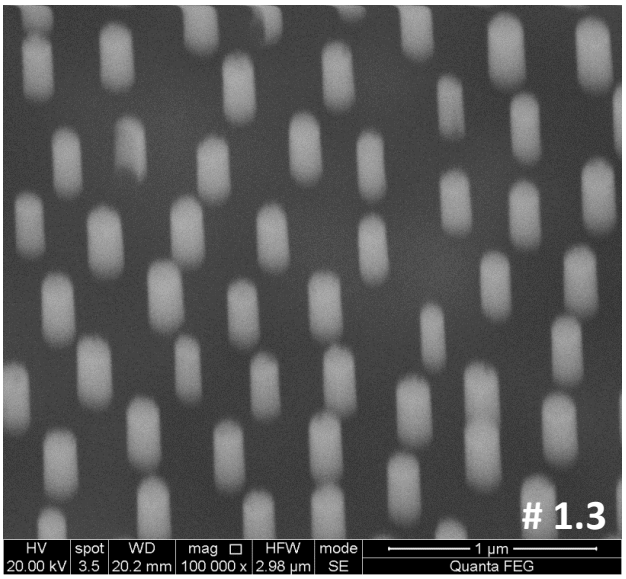

ANNEX IMAGE 3. IMAGE OF SILICON NANOPILLARS (SAMPLE #1.3). SCALE = 1 µm

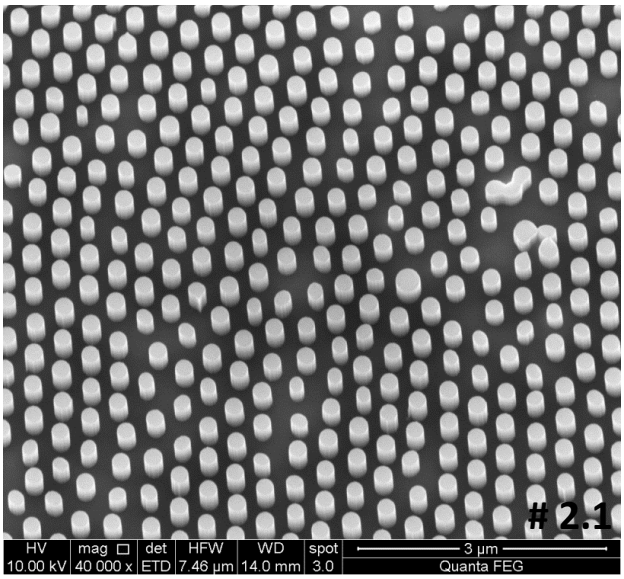

ANNEX IMAGE 4. IMAGE OF SILICON NANOPILLARS (SAMPLE #2.1). SCALE = 3 µm

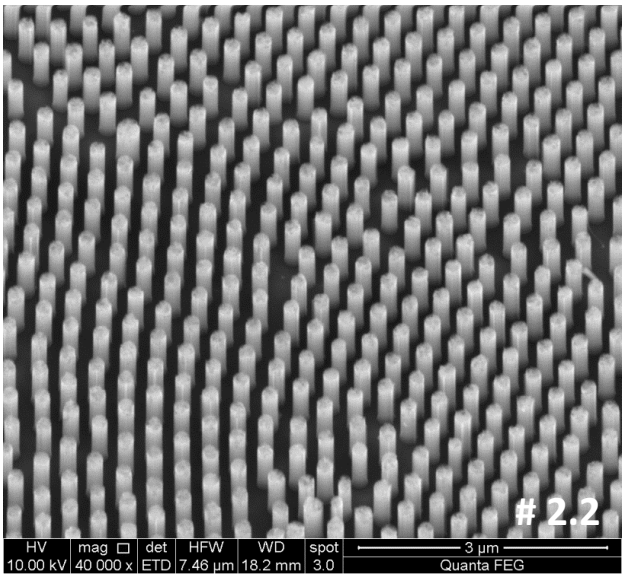

ANNEX IMAGE 5. IMAGE OF SILICON NANOPILLARS (SAMPLE #2.2). SCALE = 3 µm

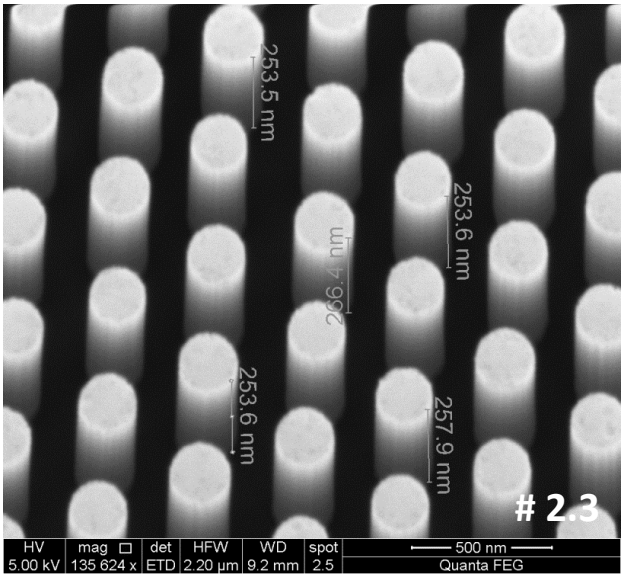

ANNEX IMAGE 6. IMAGE OF SILICON NANOPILLARS (SAMPLE #2.3). SCALE = 500 nm

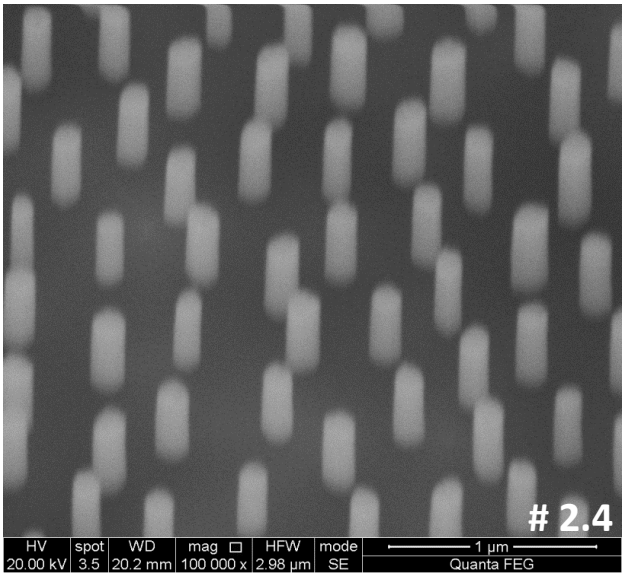

ANNEX IMAGE 7 IMAGE OF SILICON NANOPILLARS (SAMPLE #2.4). SCALE = 1 µm

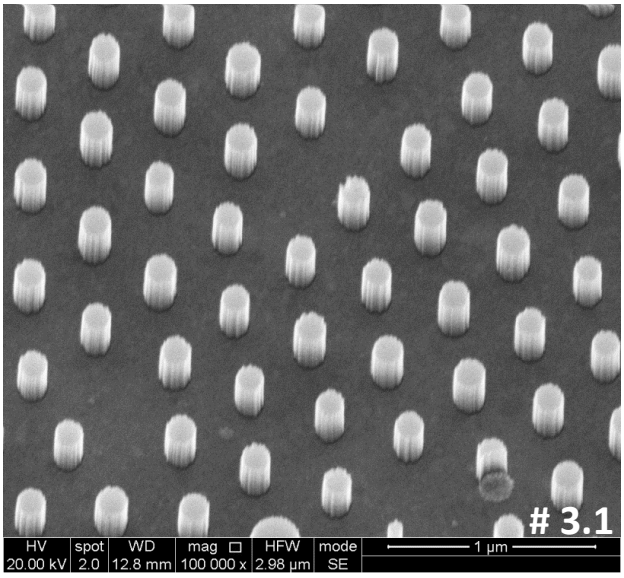

ANNEX IMAGE 8. IMAGE OF SILICON NANOPILLARS (SAMPLE #3.1). SCALE = 1 µm

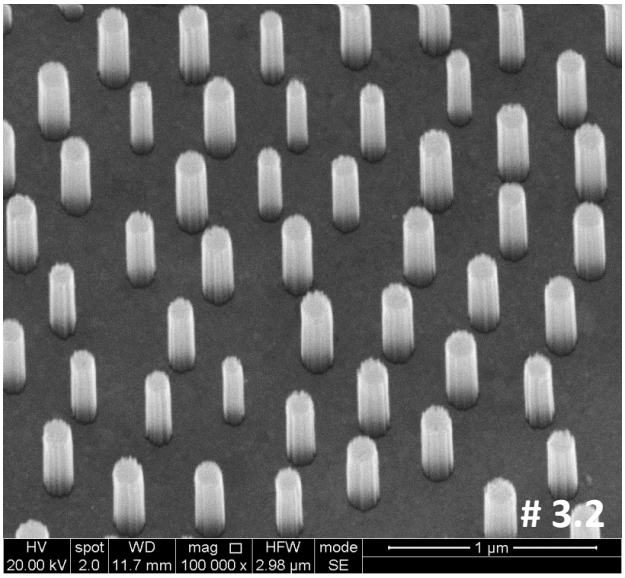

ANNEX IMAGE 9. IMAGE OF SILICON NANOPILLARS (SAMPLE #3.2). SCALE = 1 µm

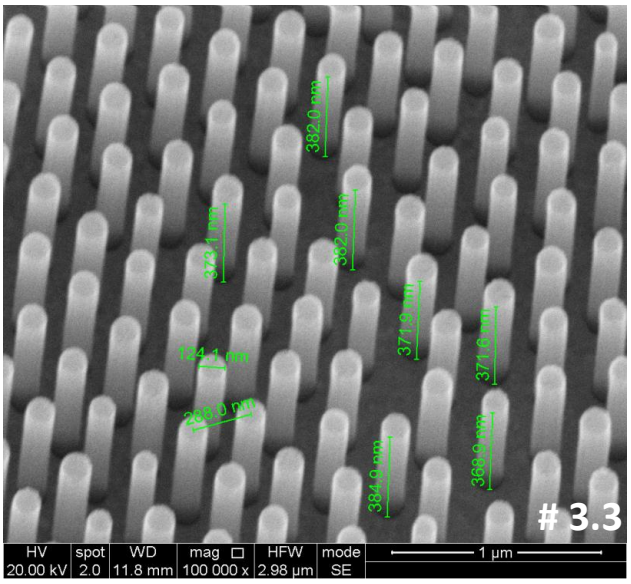

ANNEX IMAGE 10. IMAGE OF SILICON NANOPILLARS (SAMPLE #3.3). SCALE = 1 µm

2. POLYMER NANOPILLARS REPLICA (SEM IMAGES)

Sample #1.1 (Polymer: EPO-TEK® OG142-87)

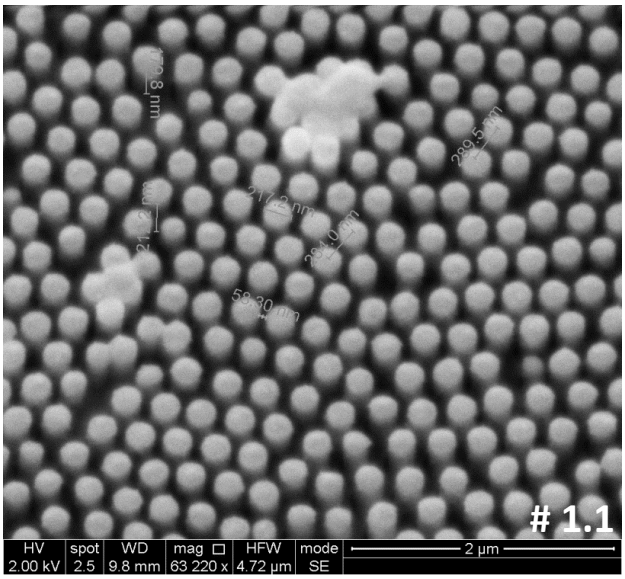

ANNEX IMAGE 11. IMAGE OF POLYMER NANOPILLARS REPLICA USING EPO-TEK® OG142-87 (SAMPLE #1.1)

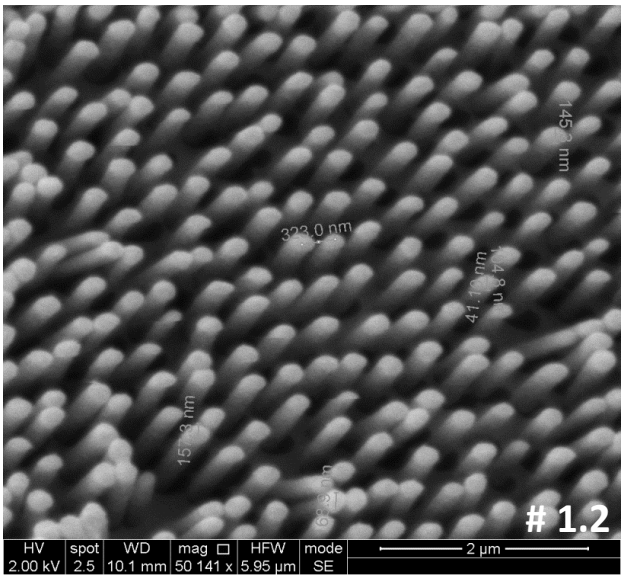

ANNEX IMAGE 12. IMAGE OF POLYMER NANOPILLARS REPLICA USING EPO-TEK® OG142-87 (SAMPLE #1.2)

Sample #1.3 **(Polymer:** EPO-TEK® OG603)

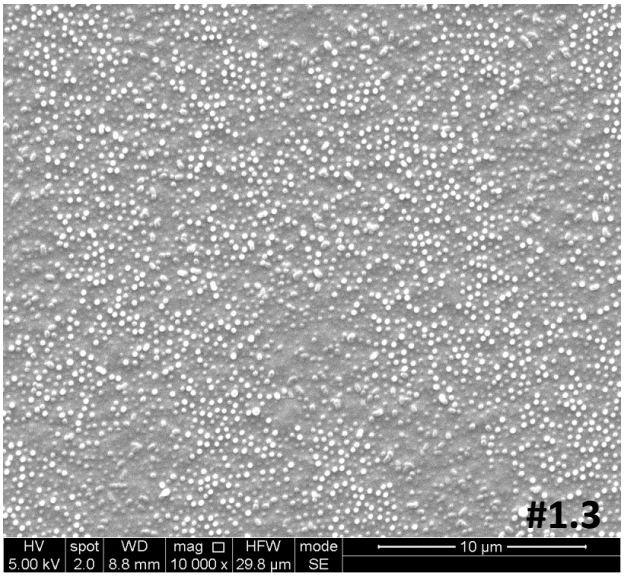

ANNEX IMAGE 13. IMAGE OF POLYMER NANOPILLARS REPLICA USING EPO-TEK® OG603 (SAMPLE #1.3)

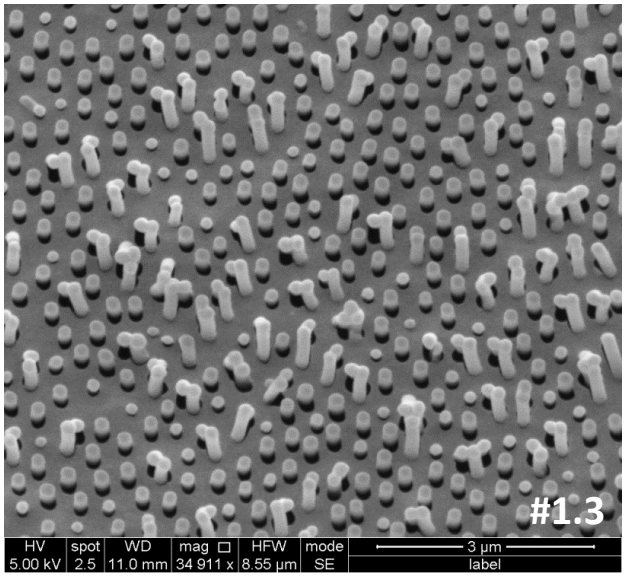

ANNEX IMAGE 14. IMAGE OF POLYMER NANOPILLARS REPLICA USING EPO-TEK® OG603 (SAMPLE #1.3)

Samples #2.1 and #2.3 **(Polymer:** EPO-TEK® OG142-87)

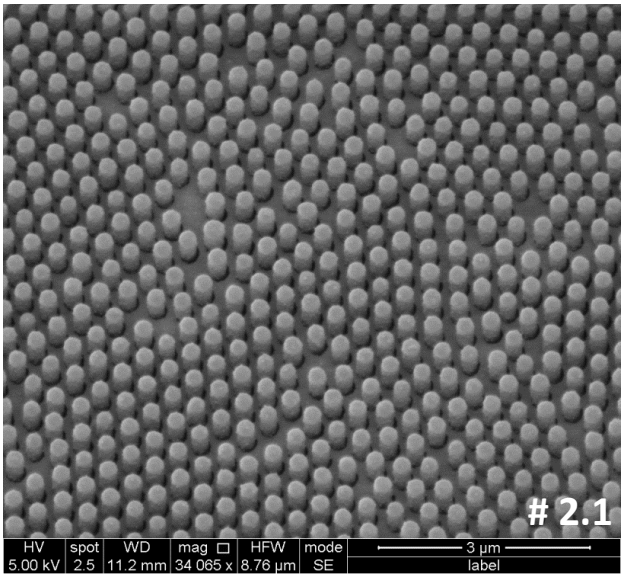

ANNEX IMAGE 15. IMAGE OF POLYMER NANOPILLARS REPLICA USING EPO-TEK® OG142-87 (SAMPLE #2.1)

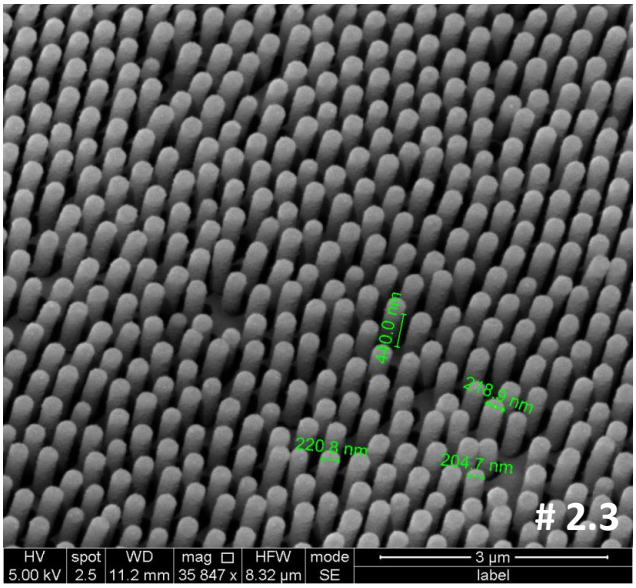

ANNEX IMAGE 16. IMAGE OF POLYMER NANOPILLARS REPLICA USING EPO-TEK® OG142-87 (SAMPLE #2.3)

Sample #2.4 (**Polymer:** EPO-TEK® OG142-87)

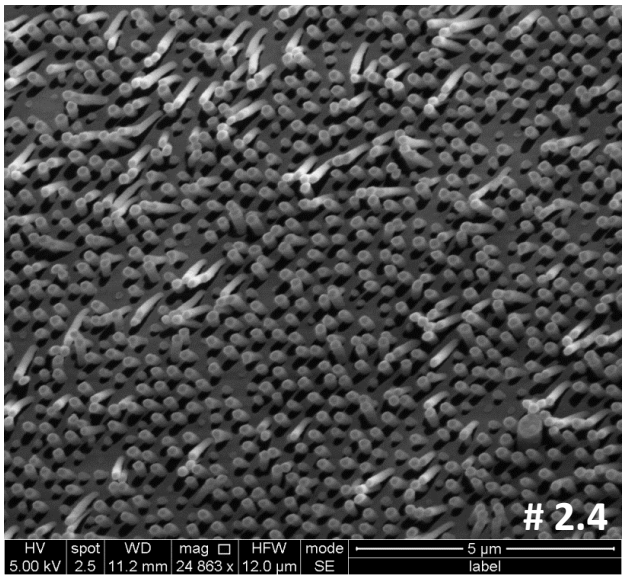

ANNEX IMAGE 17. IMAGE OF POLYMER NANOPILLARS REPLICA USING EPO-TEK® OG142-87 (SAMPLE #2.4)

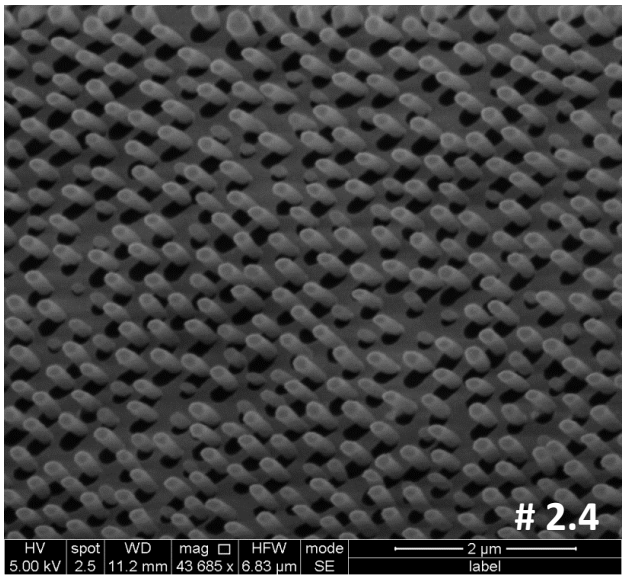

ANNEX IMAGE 18. IMAGE OF POLYMER NANOPILLARS REPLICA USING EPO-TEK® OG142-87 (SAMPLE #2.4)

Sample #2.1 (**Polymer:** EPO-TEK® OG603)

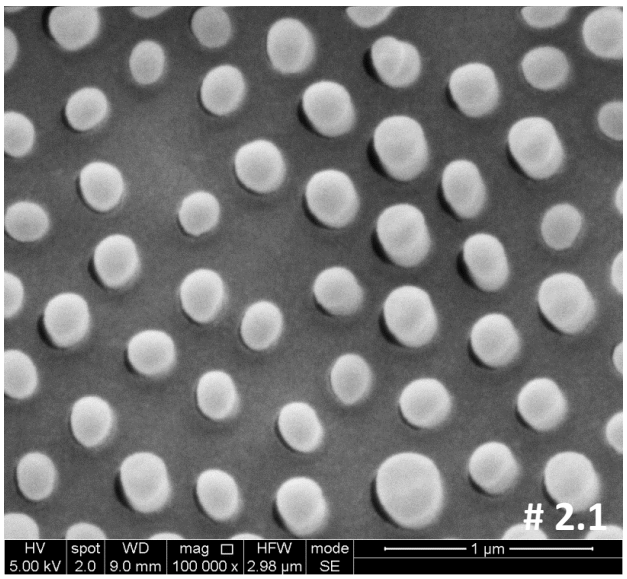

ANNEX IMAGE 19. IMAGE OF POLYMER NANOPILLARS REPLICA USING EPO-TEK® OG603 (SAMPLE #2.1)

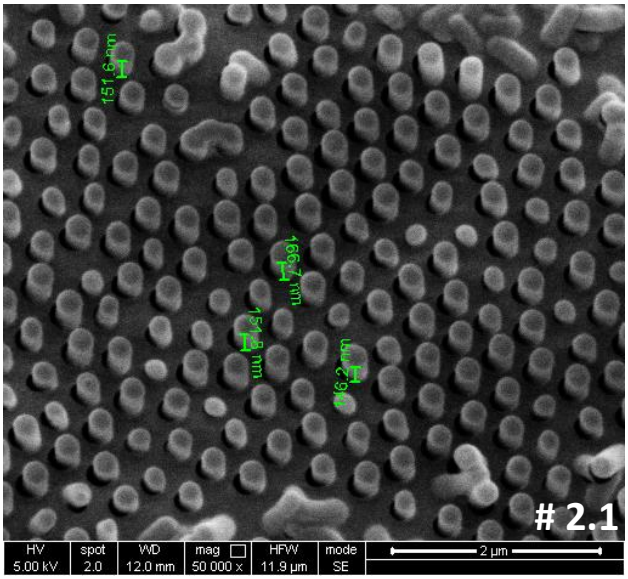

ANNEX IMAGE 20. IMAGE OF POLYMER NANOPILLARS REPLICA USING EPO-TEK® OG603 (SAMPLE #2.1)

Sample #3.1 (Polymer: EPO-TEK® OG142-87)

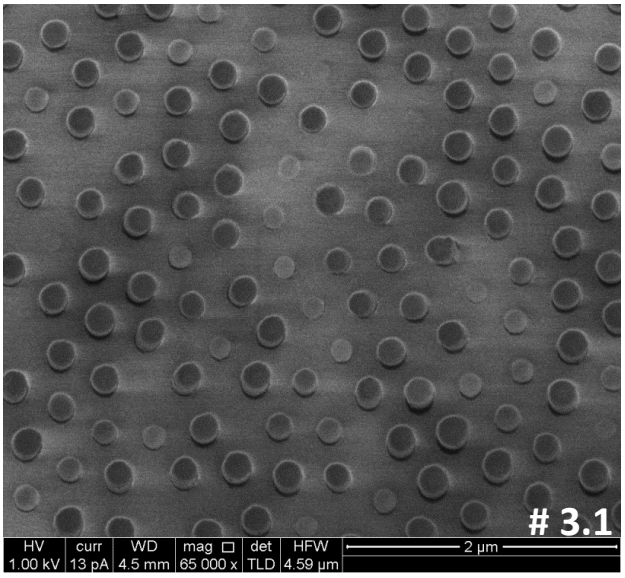

ANNEX IMAGE 21. IMAGE OF POLYMER NANOPILLARS REPLICA USING EPO-TEK® OG142-87 (SAMPLE #3.1)

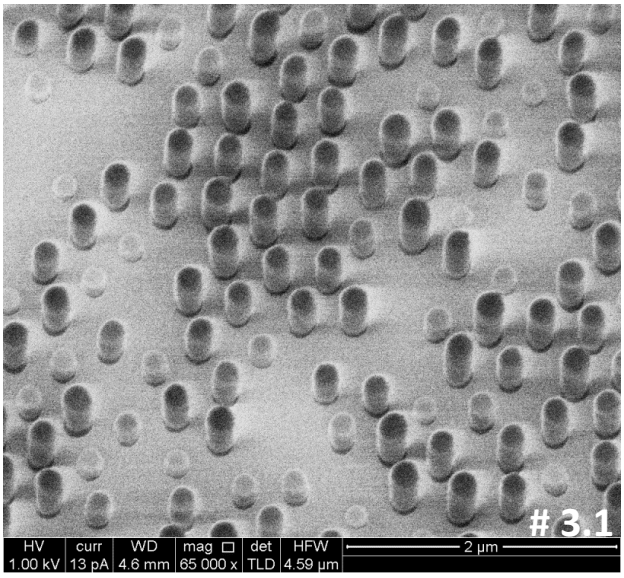

ANNEX IMAGE 22. IMAGE OF POLYMER NANOPILLARS REPLICA USING EPO-TEK® OG142-87 (SAMPLE #3.1)

Sample #3.2 (Polymer: EPO-TEK® OG603)

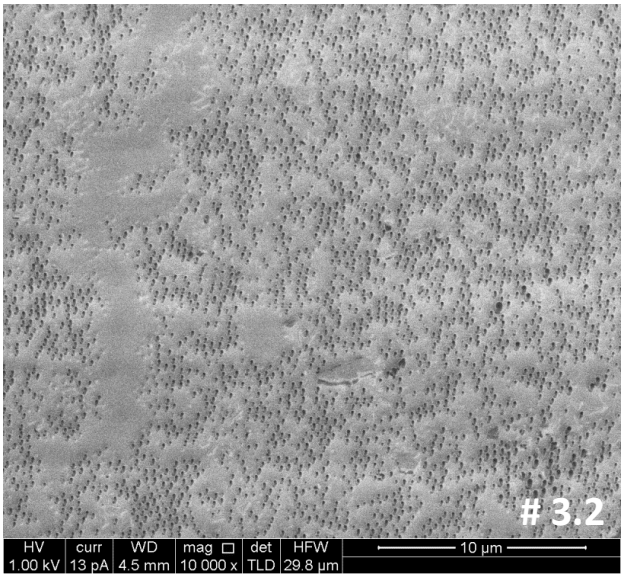

ANNEX IMAGE 23. IMAGE OF POLYMER NANOPILLARS REPLICA USING EPO-TEK® OG603 (SAMPLE #3.2)

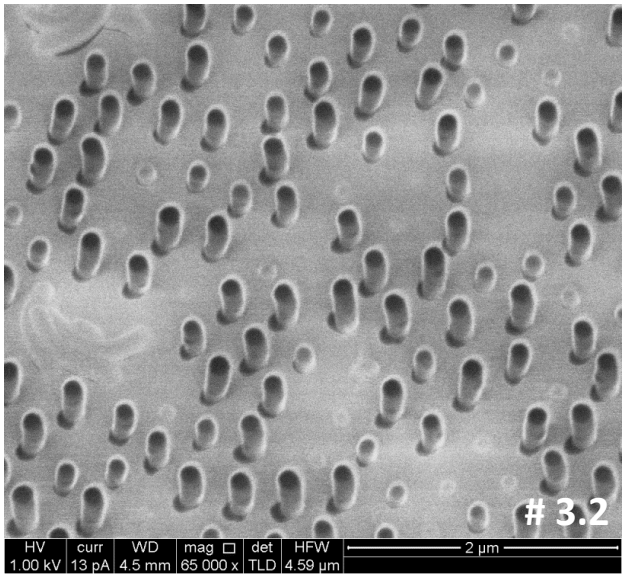

ANNEX IMAGE 24. IMAGE OF POLYMER NANOPILLARS REPLICA USING EPO-TEK® OG603 (SAMPLE #3.2)

3. NANOPILLAR DIMENSION HISTOGRAMS

Sample #1.3 Replication (Polymer: EPO-TEK® OG142-87)

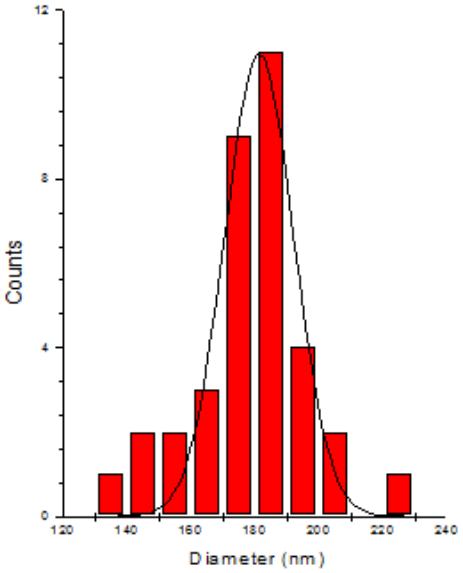

ANNEX FIGURE 1. HISTOGRAM OF NANOPILLAR DIAMETER (SAMPLE #1.3, EPO-TEK® OG142-87). IN BLACK, THE ADJUST TO A GAUSSIAN FUNCTION.

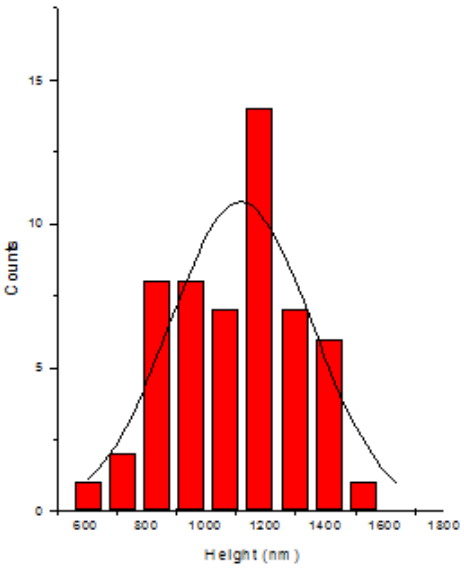

ANNEX FIGURE 2. HISTOGRAM OF NANOPILLAR HEIGHT (SAMPLE #2.1, EPO-TEK® OG142-87). IN BLACK, THE ADJUST TO A GAUSSIAN FUNCTION

Sample #2.1 Replication (Polymer: EPO-TEK® OG142-87)

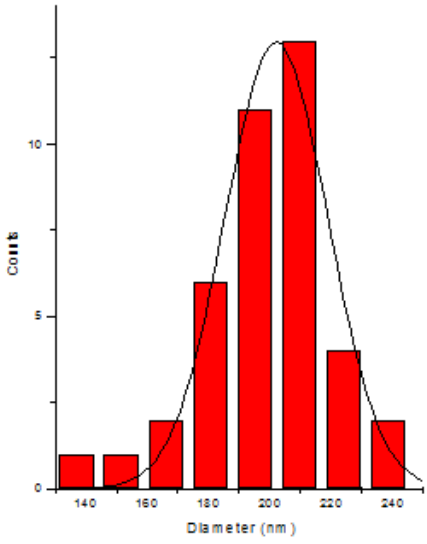

ANNEX FIGURE 3. HISTOGRAM OF NANOPILLAR DIAMETER (SAMPLE #2.1, EPO-TEK® OG142-87). IN BLACK, THE ADJUST TO A GAUSSIAN FUNCTION.

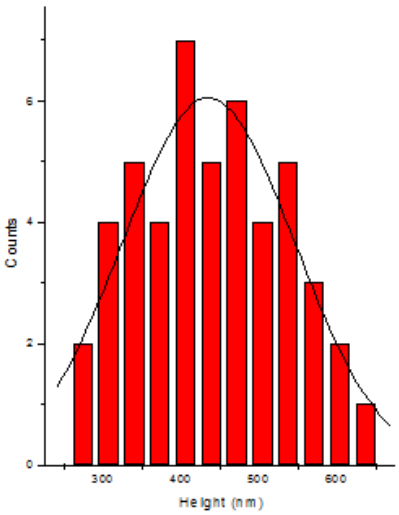

ANNEX FIGURE 4. HISTOGRAM OF NANOPILLAR HEIGHT (SAMPLE #2.1, EPO-TEK® OG142-87). IN BLACK, THE ADJUST TO A GAUSSIAN FUNCTION.

Sample #2.2 Replication (Polymer: EPO-TEK® OG142-87)

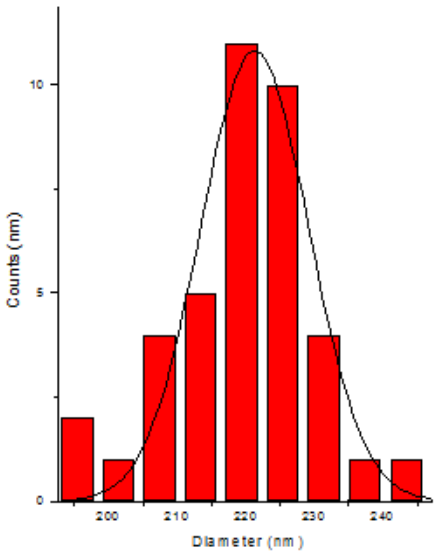

ANNEX FIGURE 5. HISTOGRAM OF NANOPILLAR DIAMETER (SAMPLE #2.2, EPO-TEK® OG142-87). IN BLACK, THE ADJUST TO A GAUSSIAN FUNCTION.

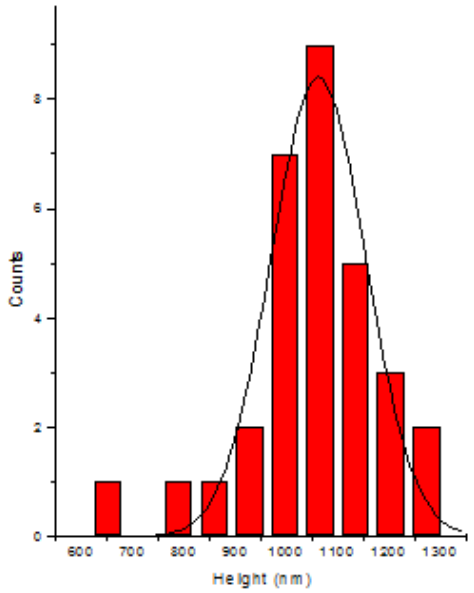

ANNEX FIGURE 6. HISTOGRAM OF NANOPILLAR HEIGHT (SAMPLE #2.2, EPO-TEK® OG142-87). IN BLACK, THE ADJUST TO A GAUSSIAN FUNCTION.

Sample #2.1 Replication (Polymer: EPO-TEK® OG603)

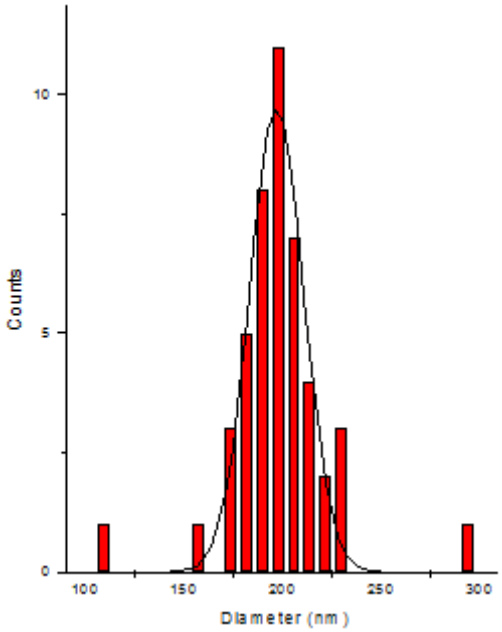

ANNEX FIGURE 7. HISTOGRAM OF NANOPILLAR DIAMETER (SAMPLE #2.1, EPO-TEK® OG603). IN BLACK, THE ADJUST TO A GAUSSIAN FUNCTION.

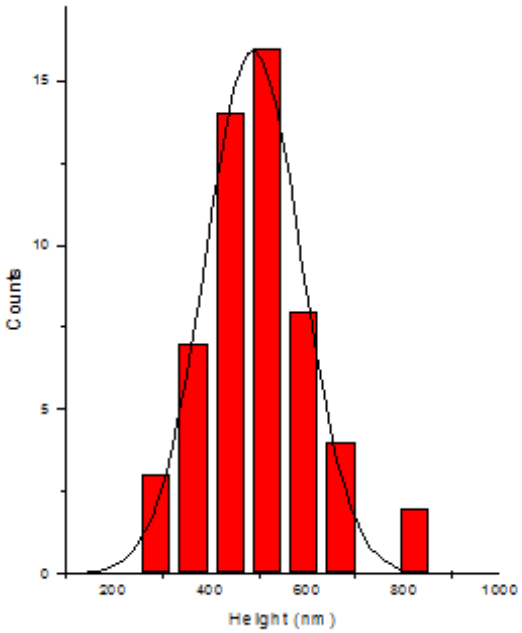

ANNEX FIGURE 8. HISTOGRAM OF NANOPILLAR HEIGHT (SAMPLE #2.1, EPO-TEK® OG603). IN BLACK, THE ADJUST TO A GAUSSIAN FUNCTION.

Sample #2.2 Replication (Polymer: EPO-TEK® OG603)

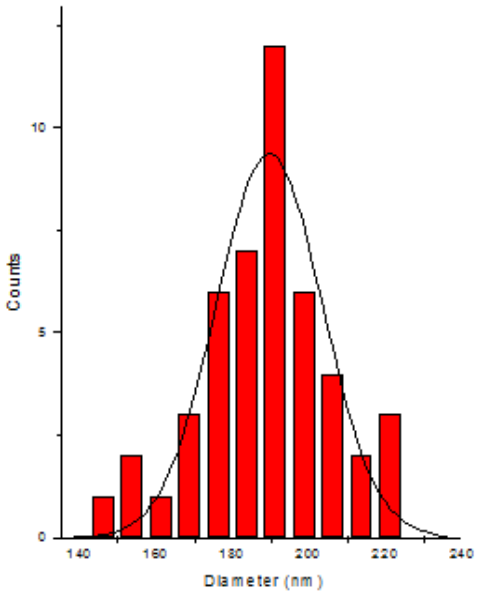

ANNEX FIGURE 9. HISTOGRAM OF NANOPILLAR DIAMETER (SAMPLE #2.2, EPO-TEK® OG603). IN BLACK, THE ADJUST TO A GAUSSIAN FUNCTION.

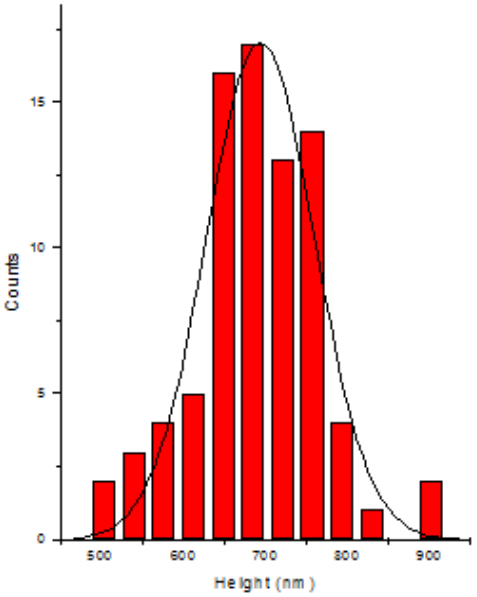

ANNEX FIGURE 10. HISTOGRAM OF NANOPILLAR HEIGHT (SAMPLE #2.2, EPO-TEK® OG603). IN BLACK, THE ADJUST TO A GAUSSIAN FUNCTION.

4. PEPTIDE DATA-SHEET

	ECV	KV
Isoelectric point (pI)	pH 4.03	pH 10.72
Net charge @pH 7	-5	+5
Sequence	Acetyl-EVSALEKEVSALEKENSALEWEVSALEKC-Amide	Acetyl-KVSALKEKVSALKEKNSALKW-KVSALKE-Amide
Estimated K_d:	$1.11 \pm 0.19 \cdot 10^{-6}$ M [pH 7, 20ºC, in PBS 10mM]	
Helical Wheel Diagram